

Solar-Terrestrial Centre of Excellence Annual Report 2015





Solar-Terrestrial Centre of Excellence

<http://stce.be/>

Ringlaan 3

B-1180 Brussels

Tel.: +32 2 373 0211

Fax: + 32 2 374 9822

Front-page: *Despite cloudy weather, the solar eclipse of 20 March was certainly one of the media highlights of 2015. Hundreds of school children found their way to the Planetarium to observe the event. But also the Space Pole got frequently visited by schools. The High School of Twente visited the premises on 20 May (top left), there were about 100 10-year-old kids from the German speaking community on 13 November (bottom left, in SSCC room), and another 100 students participated in the ASGARD-project (experiments launched with the RMI balloon; top right).*

Table of Contents

Preface.....	4
Structure of the STCE	5
Monitoring Space Weather: Solar-Terrestrial Highlights in 2015.....	8
Public Outreach meets Science	12
ESWW: Belgian wins an award!.....	12
A science party for everyone!	13
SOHO 20 years!	14
The STCE Annual Meeting	16
Fundamental Research.....	18
The sunspot number's new clothes	18
Time variability of Integrated Water Vapour content.....	19
Plasma turbulence and ion beams in the solar wind.....	20
Instrumentation and experiments	23
Pilot Network for Identification of TIDs in Europe	23
Ionosonde observations of the 20 March 2015 solar eclipse.....	25
Total Solar Irradiance.....	26
PICASSO-SLP, a space weather instrument for a scientific nano-satellite.....	27
Applications, Modeling and Services	30
Automatic detection of CMEs in Heliospheric Imager data	30
Sunny views with jHelioviewer	31
PARAFOG: using ALC to forecast radiation fog	33
Natural Hazard Assessment for Aviation	34
Publications.....	38
Peer reviewed articles.....	38
Presentations and posters at conferences.....	42
Public Outreach: Talks and publications for the general public	52
List of abbreviations	54

Preface

Dear reader,

Since its foundation in 2006, the Solar-Terrestrial Centre of Excellence has undergone enormous changes. It evolved to a true centre of excellence with a leading role in the Sun-Space-Earth landscape, a high standard for research and an effective service centre for the government, society and industry. This annual report proves that we are on the track that we had envisioned.

And we will continue doing this.

I hope that -while reading this report- you can feel our enthusiasm. And maybe we meet at one of our future activities.



Ronald Van der Linden
General Coordinator of the Solar-Terrestrial Centre of Excellence
Director General of the Royal Observatory of Belgium

Structure of the STCE

The Solar-Terrestrial Centre of Excellence is a project of scientific collaboration that focuses on the Sun, through interplanetary space, up to the Earth and its atmosphere.

The solid base of the STCE is the expertise that exists in the 3 Federal Scientific Institutes of the Brussels Space Pole: the Royal Observatory of Belgium, the Royal Meteorological Institute and the Belgian Institute for Space Aeronomy. The STCE supports fundamental solar, terrestrial and atmospheric physics research, is involved in earth-based observations and space missions, offers a broad variety of services (mainly linked to space weather and space climate) and operates a fully established space weather application centre. The scientists act at different levels within the frame of local, national and international collaborations of scientific and industrial partners.

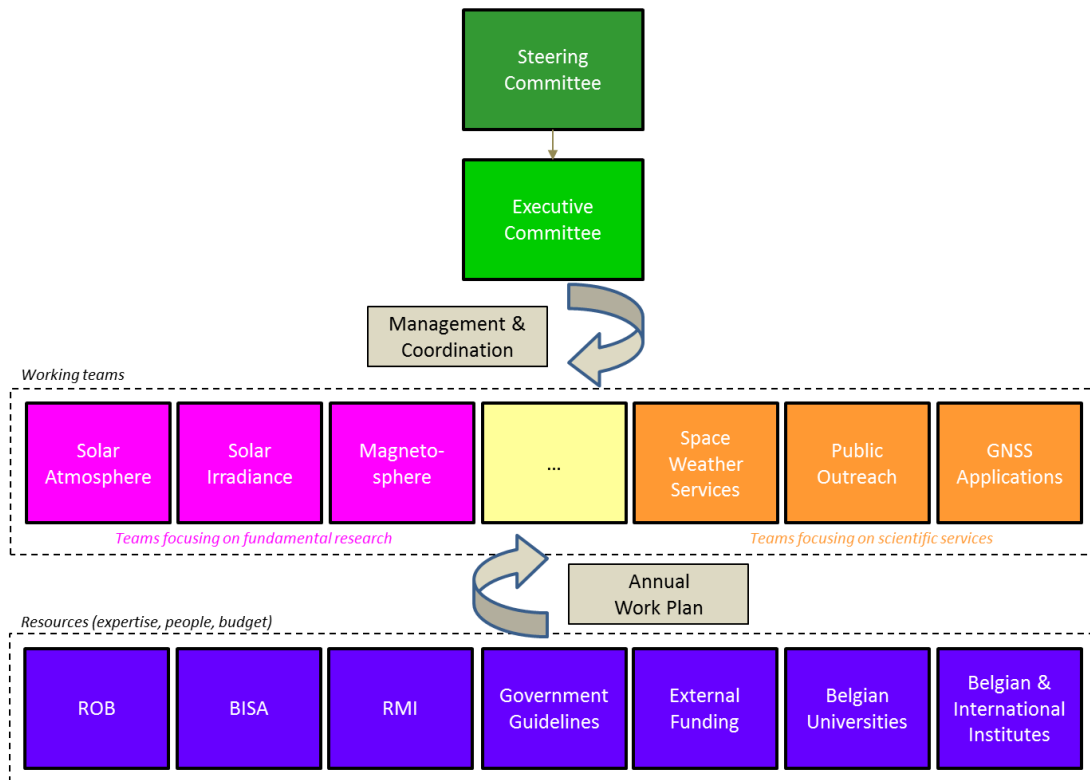


Figure 1: The STCE management structure

The STCE's strengths are based on sharing know-how, manpower, and infrastructure.

In order to optimize the coordination between the various working groups and institutions, as well as the available resources such as ICT, personnel and budget, a management structure for the STCE was put into place, consisting of a steering committee and an executive committee.

The **steering committee** takes all the final decisions on critical matters with regard to the STCE. It assures the integration of the STCE into the 3 institutions and the execution of the strategic plans. It is composed of:

- BELSPO Director General “Research Programs and Applications”

Dr. Frank Monteny (BELSPO)

- Director General of each of the 3 institutions at the Space Pole

Dr. Ronald Van der Linden (ROB)

Dr. Daniel Gellens (RMI)

Dr. Martine De Mazière (BISA)

The **executive committee** assures the global coordination between the working groups and the correct use of the budgetary means for the various projects. It also identifies new opportunities and is the advisory body to the Steering Committee. It is composed of:

- STCE Coordinator

Dr. Ronald Van der Linden

- Representatives of the research teams in the 3 institutes

Dr. David Berghmans (ROB)

Dr. Carine Bruyninx (ROB)

Dr. Johan De Keyser (BISA)

Dr. Michel Kruglanski (BISA)

Dr. Stanimir Stankov (RMI)

Dr. Steven Dewitte (RMI)

Dr. Hugo De Backer (RMI)

A promotional movie giving a flavor of the STCE’s tasks, interactions and various research programs can be found via the [STCE](#) website (in [English](#), and subtitled in [French](#) and [Dutch](#)).



Figure 2: Space Pole residents are enjoying sweet refreshments from the ice cream car, which quickly became a familiar and well appreciated sight on the plateau.

Monitoring Space Weather: Solar-Terrestrial Highlights in 2015

The official annual sunspot number (SN) for 2015, as determined by the [WDC-SILSO](#) (World Data Centre - Sunspot Index and Long-term Solar Observations), was 69.8. This is a 38% decrease compared to 2014, when it was 113.3 and the maximum of the ongoing solar cycle (SC24) was reached.

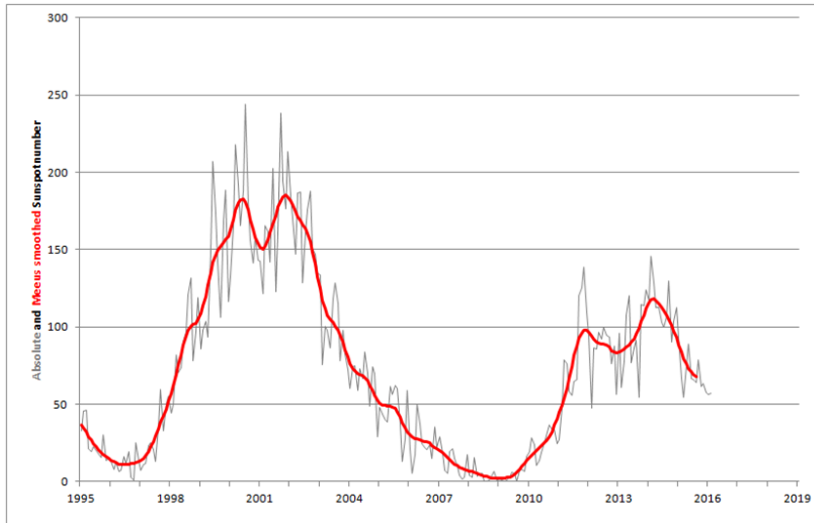


Figure 3: The evolution of the monthly and monthly smoothed SN (1995-2015). Pending the smoothing formula used, SC24 reached its maximum of 116.4 in April 2014 (SILSO formula), or 118.2 in March 2014 (Meeus formula).

Note that on 1 July 2015, SILSO introduced the new version of the international sunspot number. See the [press release](#) and further details on page 18 of this annual report. Unless otherwise noted, it is this latest version of the SN that is being used throughout this document.

In 2015, the highest daily sunspot number was 172 and recorded on 13 May. There were no spotless days.

Throughout the year, sunspot activity was driven by both solar hemispheres, with no particular persistent dominance noted from any of the hemispheres. The largest sunspot groups were [NOAA 2403](#) and NOAA 2371, both reaching about 7 times the total surface area of the Earth. For a reference: Famous sunspot region [NOAA 2192](#) (October 2014) reached nearly 16 times our planet's surface area...

The year 2015 will probably best be remembered for the two strong geomagnetic storms that it produced, in fact the strongest so far of SC24. The first severe storm took place on 17 March and was aptly named the [Saint Patrick Day's geomagnetic storm](#). Its source was a 2-hour long C9 flare on 15 March produced by NOAA 2297. This sunspot region supremely ruled the solar activity from 5 till 20 March, and despite its modest size became the most flare active region of the year. It produced more than 20 M-class flares and an [X2.2 flare](#) on 11 March.

The partial halo coronal mass ejection (CME) associated with the 15 March flare had an earth-directed component and hit Earth early on Saint Patrick's day, sparking the most intense geomagnetic storm of the current solar cycle ($K_p = 8$; $Dst = -223$ nT)

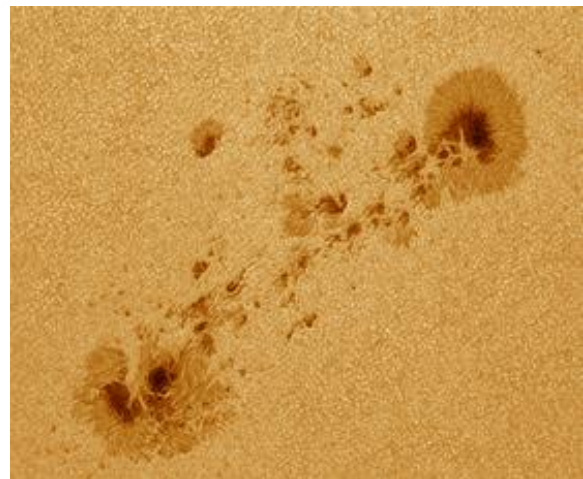


Figure 4: NOAA 2403 was one of the largest sunspot groups of the year and visible during the summer holidays. Hence, for two weeks, it became the most photographed feature on the Sun. Leo Aerts from the Belgian Astronomical Association took this picture on 23 August using a 14 cm telescope.

so far. Aurora were visible from countries well south of the usual polar light regions, with polar lights photographed and reported from France (Vosges, Picardy,...), Germany, the Czech Republic, and the middle of Russia. The passing CME temporarily reduced the cosmic rays arriving at Earth, and a Forbush decrease (i.e. a rapid decrease in the observed galactic cosmic ray intensity) of 4.5% was recorded by neutron monitors on Earth ([Oulu NM](#)).

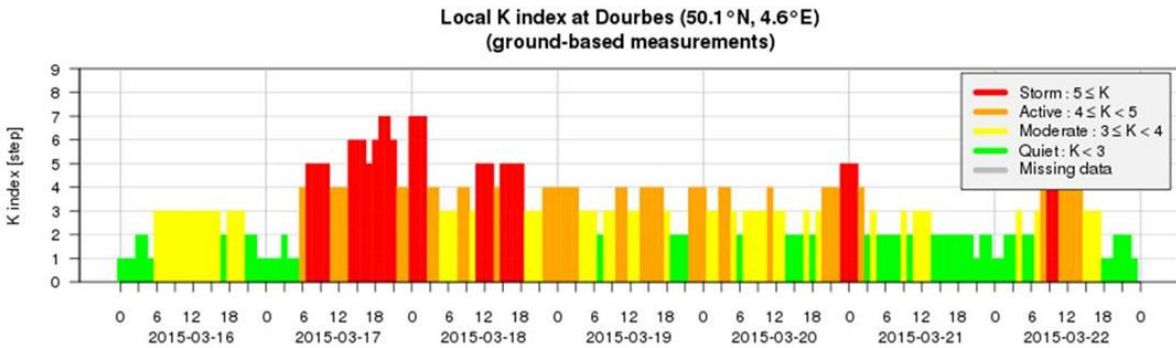


Figure 5: The strong geomagnetic disturbance of 17 March was also observed by magnetometers in [Dourbes](#) where a major storm ($K = 7$) was recorded.

A very similar scenario unfolded during the last 10 days of June (18-27 June) when NOAA 2371, one of the largest sunspot groups in 2015 unleashed all its fury. A double M-class flare early on 21 June and two strong M-class flares on [22 and 25 June](#) resp. were associated with full halo CMEs. This resulted in a severe geomagnetic storm on 22 June (the “[Solstice storm](#)”; $K_p = 8$, $Dst = -204$ nT) which was the second strongest of the year after the 17 March storm. B_z reached an unusual -37 nT, the most negative excursion measured in 2015. So far this solar cycle, no extremely severe geomagnetic storm has been observed ($K_p = 9$).

The quick succession of passing CMEs temporarily reduced once again the cosmic rays arriving at Earth, and a Forbush decrease of nearly 8% was recorded, the strongest of 2015 ([Oulu NM](#)). It took nearly a week before neutron counts were back at nominal level. The 21 June flares were most likely also responsible for the strongest proton event of the year, a strong solar radiation storm ([S3](#)). The peak of this radiation storm [coincided](#) with the peak of the severe geomagnetic storm and the M6 flare, around 19:00UT on 22 June.

In between these storms, on 5 May, the strongest flare of the year was observed. Little did space weather forecasters know that this would also be the last X-class solar flare of the year! It concerned a relatively modest [X2.7 flare](#) barely lasting 10 minutes. The source region, NOAA 2339, was one of the larger sunspot groups of the year but produced

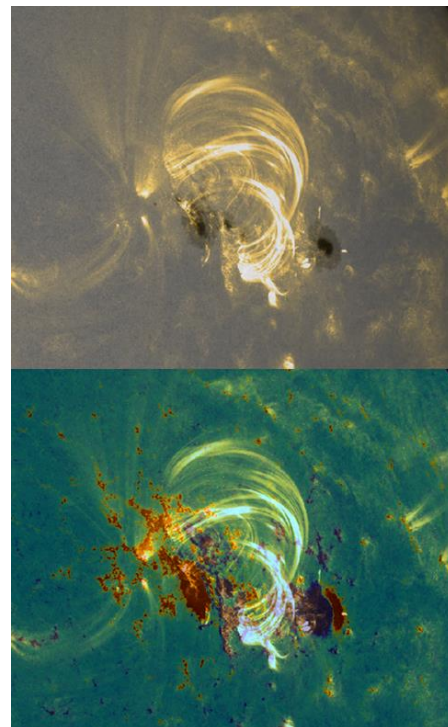


Figure 6: A view on the post-flare coronal loops after the M7 flare on 25 June. The SDO/AIA 171 image has been overlaid on a white light image (top) and on a magnetogram (bottom).

mostly C-class flares. The associated, fast CME was not directed to Earth. So far, only 45 X-class flares have been recorded during SC24 – that’s quite a bit less than the 126 events during SC23!

Fortunately, the number of M-class flares was well living up to expectations, with over 100 recorded. Some were simply photogenic, while others highlighted particular features of a typical solar flare, such as coronal loops, transient coronal holes, or plasma ejections. In 2015, just 5 groups were responsible for both X-class flares, about 60% of all M-class flares, and 25% of all C-class events: Compact NOAA

2297, and the 4 largest sunspot regions NOAA 2339, 2371, 2403 and [2422](#).

On 4 November, NOAA 2443 produced an [M3.7 flare](#) peaking at 13:39UT. This at first sight very normal flare was associated with strong radio and ionospheric disturbances that also affected radar and GPS frequencies. As a result, Swedish air traffic was halted for about an hour during the afternoon. The air traffic problems started at the most intense phase of the radio storm, and followed right on the heels of a minor geomagnetic storm caused by the high speed stream of a coronal hole (CH). The CME associated with the M3 flare would cause a moderate ($K_p = 6$) geomagnetic storm during the first half of 7 November.

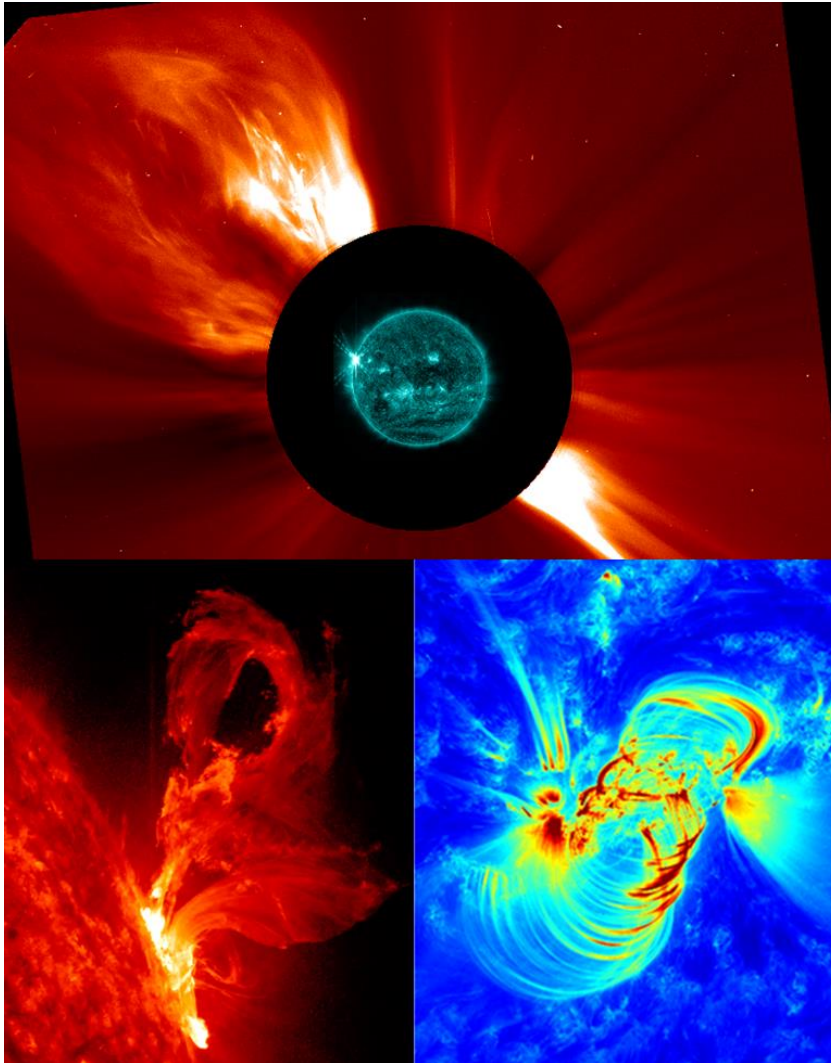


Figure 7: (top) A composition of the X2 flare from NOAA 2339 on 5 May as seen in EUV (22:17UT) and a coronagraphic image from SOHO/LASCO C2 55 minutes later (23:12UT) showing the full extent of the associated CME. (bottom left) The modest M3.7 flare on 2 March was produced by [NOAA 2290](#) and got accompanied by an impressive and dynamic ejection of plasma. (bottom right) This is a false color image from post-flare coronal loops following the M1.8 flare in [NOAA 2473](#) on 28 December. It was associated with a proton enhancement (no event), a lovely arcade (series of post-flare coronal loops), a number of jets near the main spot, and a CME that would lead to a moderate geomagnetic storm as Earth entered a New Year.

There were plenty of prominence and filament eruptions in 2015! Prominences are regions of dense and relatively cool material that are squeezed between fields of opposite magnetic polarity, having typical values for height and

length of resp. 30.000 km and 100.000 km. Some of the specimens grew to extraordinary sizes before erupting, such as the prominence that erupted on [27 March](#), which was more than 8 times as tall as the

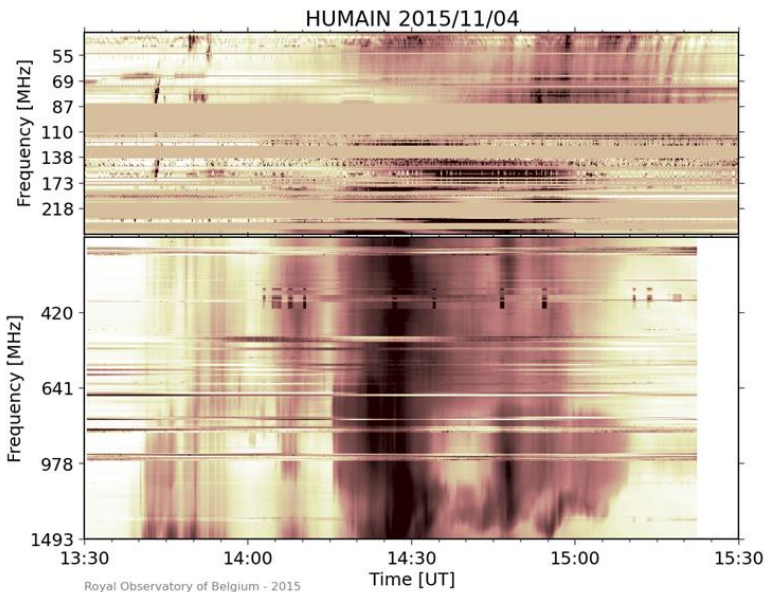


Figure 8: The effect of the 4 November M3 flare on radio frequencies was nicely recorded by the Humain Solar Radio Spectrograph (HSRS). The radio spectrogram or dynamic spectrum (recorded by HSRS) is a graphical presentation of the blue emission intensity, with on the horizontal x-axis time (increasing from left to the right) and on the vertical y-axis the frequency (increasing from top to bottom). The HSRS observations are unique radio observations in Europe, covering a rather large frequency range.

celebrating their [20th anniversary](#) on 2 December.

Of note was also the [very fast solar wind](#) that was recorded early October. For nearly 3.5 days, solar wind speed at Earth was over 500 km/s. Peak speeds of 810 km/s and more were recorded late on 7 and early on 8 October. The source of the raging solar wind was a trans-equatorial coronal hole that transited the central meridian early on 5 October. High solar wind speeds (more than 800 km/s) near Earth are rare, happening only twice in 2015 – the other one being on 27 June. Large coronal holes were also observed late January (south pole extension) and early December (north pole extension). Meanwhile, the aging ACE spacecraft is still the prime monitor of the solar wind, but it got accompanied by the fresh [DISCOVER](#) satellite which was launched on 11 February. It reached its final orbit at the L1 point on 8 June and will be the future replacement of ACE.

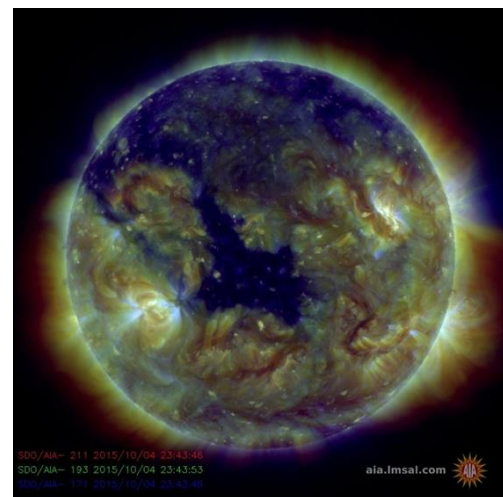


Figure 9: The trans-equatorial coronal hole that was responsible for the very high solar wind speed during early October.

Earth, and had a length of nearly the Earth-Moon distance! Other impressive eruptions took place on [24 February](#), [28 April](#), and [30 September](#). One of the filament eruptions took place on [19 July](#) and was associated with a C2 flare of very long duration. In fact, with its 3 hours and 40 minutes, it was the C-class flare with the longest duration in 2015. Moreover, it took the x-ray flux several more hours to decline back to pre-eruptive levels.

Early July, the life of space weather forecasters got a lot easier again with the [reawakening of STEREO-A](#). When a CME is observed, it can now much more accurately be determined if the plasma cloud is heading for Earth or not. Meanwhile, SOHO and its pair of coronagraphs are still going strong,

Public Outreach meets Science

ESWW: Belgian wins an award!

Since 2013, space weather has its own yearly medal award ceremony at the annual European Space Weather Week conference (ESWW). In 2015, Dr. David Berghmans won the Marcel Nicolet medal for his efforts to structure the space weather community at an international level.

The study of space weather is a young scientific discipline with increasing importance due to the impact that solar storms can have on our high-technological society.

David Berghmans stood at the cradle of the space weather program in Belgium and Europe. The study of space weather received a boost in the nineties from the joint ESA/NASA space mission Solar and Heliospheric Observatory (SOHO) to which Belgium contributed substantially with the EIT telescope. In the year 2000, David Berghmans created a Belgian Space Weather Center combining fundamental and applied research, which paved the road to space weather services and predictions up to a few days in the future. The center is one of the cornerstones of a worldwide network.



Figure 10: Dr. David Berghmans received the Marcel Nicolet Medal at the Kursaal in Oostende, Belgium.

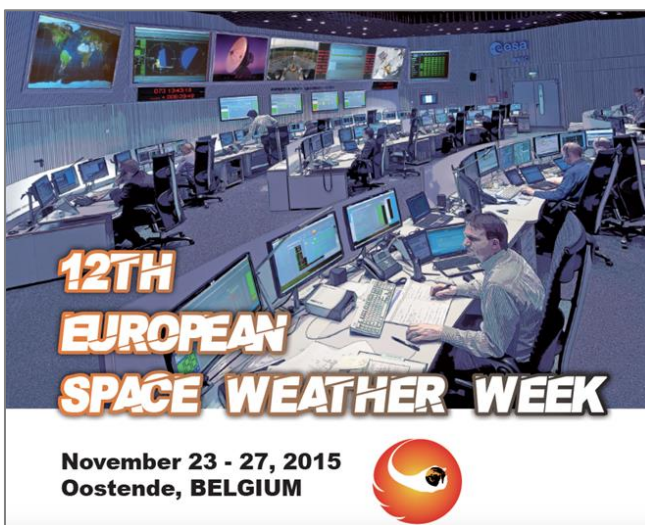


Figure 11: The organization of the 12th European Space Weather Week was in the hands of the STCE. 2015 was a top year, despite the terror threat. For five days in a row, participants could taste a variety of space weather, from “hard core” theory to physical applications, from space weather induced incidents to the latest technological innovations. If it is space weather related, you find it at ESWW.

David is a passionate, open mind solar physicist at the Royal Observatory of Belgium and involved in a long series of missions and projects that are essential in the different aspects of space weather and that strengthen the European and world space weather efforts. The trick is to recognize opportunities and pepper them with original ideas and out-of-the-box thinking. But David was also very clear in his medal speech: all his successes are rooted in the team of colleagues he’s collaborating with. His expertise in space instrumentation led his team to the micro-satellite adventure [PROBA2](#) with the state-of-the-art EUV solar imager SWAP and spectrograph LYRA. This success story continues in the form of participation in numerous other space weather projects of the 21st century, contributing to the ‘Golden Age’ of solar and heliospheric physics with missions like

PROBA3 and Solar Orbiter. Space doesn’t seem to be far away for David.

David received his award during the medal ceremony at the 12th European Space Weather Week held in Oostende. The STCE is one of the main organizers and welcomes more than 400 participants to discuss space weather questions. What is the probability that a solar storm will occur? - Will the solar panels of satellites in a geostationary orbit be damaged? - Can the Sun cause radar blackouts disrupting air traffic? What is the dose-impact for a particular technological system and how relates this to construction costs? Both commercial and scientific issues associated with space weather make part of the debate to finally come to a resilient and space weather proof society.

A science party for everyone!

On Friday, 20 March, an impressive partial solar eclipse was visible from Belgium between 9:26 LT and 11:47 LT. This eclipse could be seen in its totality only from the Faroe Islands and Svalbard (Norway), and was partial in Europe.

Witnessing a solar eclipse is a rare experience. In the past, a total eclipse was the only way to observe the immediate environment around the Sun and to get an idea of the structure and composition of the solar atmosphere. It made scientists realize how complex and extended the solar atmosphere actually is. Nowadays, we have instruments that can create an artificial eclipse on a permanent base, but they suffer from technical limitations. Hence, observing a solar eclipse using classical means remains valuable for us scientists as it allows us to calibrate our solar instruments.

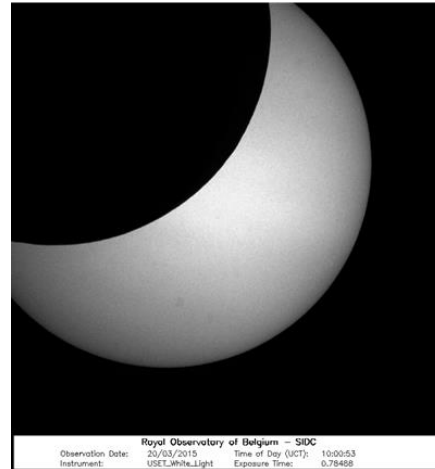


Figure 12: The clouds obstructed our view at the observation site in Uccle. We could capture only one, very nice, white light image of the eclipse with the USET telescope.

But above all, a solar eclipse offers us the opportunity to put our favorite object of study, the Sun, in the picture and to share our enthusiasm.

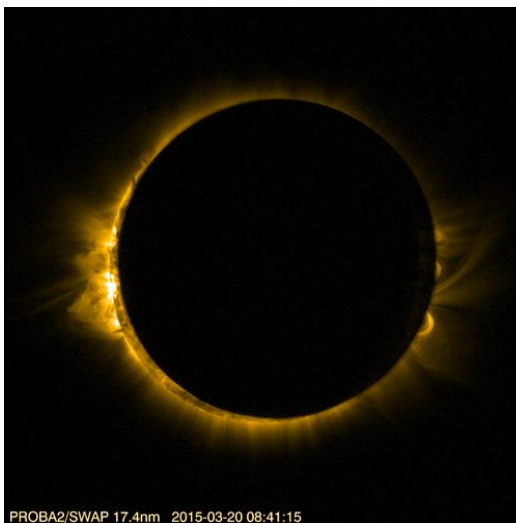


Figure 13: The solar eclipse seen from space by the satellite PROBA2. The SWAP telescope images the Sun in extreme ultraviolet (EUV) light.

We coordinated an observation campaign so that all our instruments were ready to observe the eclipse. Those that didn't have the chance to observe the eclipse themselves could follow the spectacle on the [eclipse website](#), where data, images and movies were posted as soon as they were available.

While the optical observations from ground were unfortunately plagued by the cloud cover, the radio telescopes in Humain could observe this event continuously. The PROBA2 satellite was the first to send around images from space, while other satellites were used to track changes in the ionosphere.

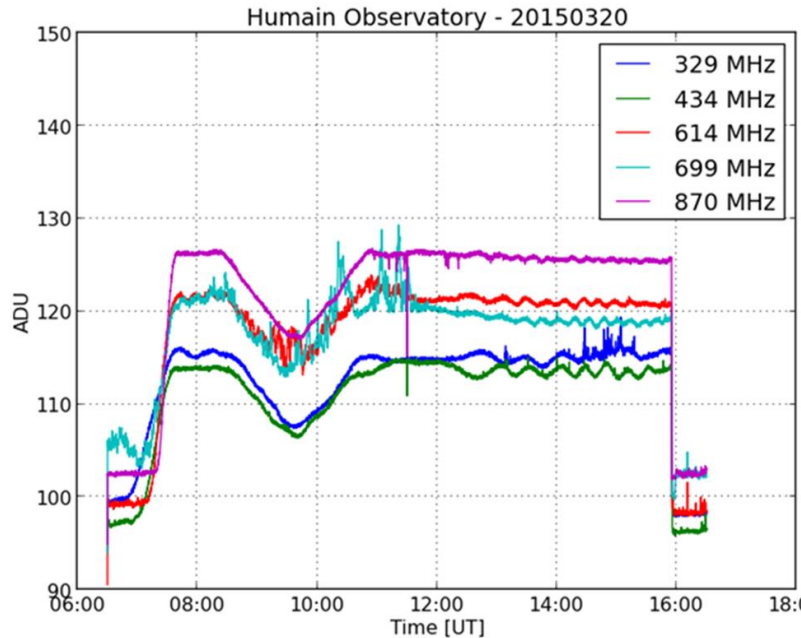


Figure 14: At the radioastronomy station Humain, we could measure the eclipse with a 6 meter dish, unhampered by the clouds. The radio light flux curves show the rise of the Sun around 07:30UT. During the eclipse, the flux decreases as the Moon passes in front of the Sun.

At the [Planetarium](#), more than 300 children and adults came together to watch the eclipse with their own eyes, through telescopes set up outside, or by looking at images streamed live from our instruments located in Uccle, Humain and from space. Our experts were happy to show and explain what an eclipse looks like when observed with radio antennas from Earth and why our satellite could observe the eclipse up to 4 times that day! The State Secretary for Science Policy, Mrs. Elke Sleurs was definitely impressed. The Planetarium was the place to be for the radio and television crews to find our visitors enthusiastically telling on how they experienced this

once-in-a-lifetime event and our experts gladly clarifying the science behind it. The March 2015 solar eclipse pictures and movies are still available at our dedicated [solar eclipse website](#).

SOHO 20 years!

On December 2, 2015 we celebrated the 20th anniversary of the launch of the ESA/NASA solar observatory “Solar and Heliospheric Observatory” (SOHO). The discoveries made by the instruments on SOHO have revolutionized solar physics and space weather worldwide (see ESA [press release](#)).

At the Royal Observatory of Belgium, the birthday of SOHO was celebrated with particular nostalgia. Indeed, the start and subsequent successes of SOHO has been the most important driver in the past 20 years behind the space activities at the “Solar Influences Data analysis Center” (SIDC), a research group of around 40 people at ROB. Together with the Centre Spatial de Liège (CSL), ROB/SIDC participated in the Extreme Ultraviolet Imaging Telescope (EIT) on SOHO.



Figure 15: The SOHO observatory was launched on 2 December 1995 as a joint ESA/NASA mission. Belgium (ROB & CSL) participated in the very successful EIT telescope thanks to BELSPO / PRODEX financing.

EIT was originally regarded as the “context imager” for the spectrographs onboard SOHO producing only 4 sets of (static) images per day, during a lifetime of 2 years. Soon however it became clear that movies of EIT images showed unexpected dynamics such as enormous ‘tsunamis’ on the Sun (which we now call EIT waves) that are related to coronal mass ejections. The SOHO mission was extended several times

and is, 20 years later, still operating a subset of the instruments, including EIT.

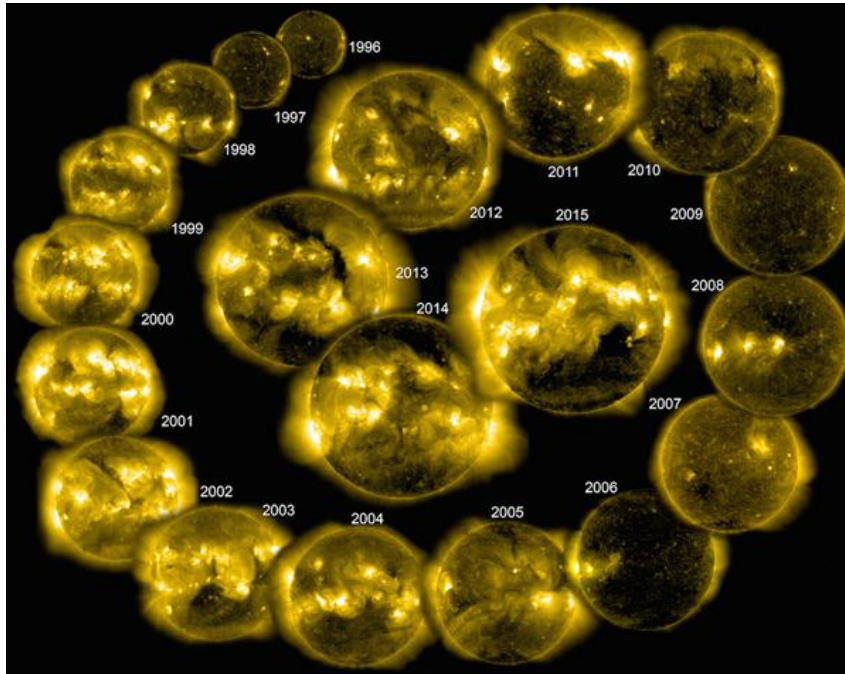


Figure 16: A snapshot per year showing the evolution of the solar corona over 2 solar cycles in the 28.4nm bandpass of EIT.

The very first generation of the post-docs at ROB/SIDC has contributed significantly in the calibration of the instrument, the science planning and the exploitation of the EIT data set. A special way of operating the telescope, the “EIT shutterless mode” was designed and pioneered at ROB. This experience brought us to the later SWAP telescope on PROBA2 and the upcoming EUVI telescopes on Solar Orbiter.

coronagraphs onboard SOHO, have been essential elements in the effort to monitor solar activity and forecast the impacts at the Earth. Also in this field, called space weather, the successes of SOHO ignited a parallel success at ROB/SIDC with the development of automated processing software and space weather activities. In this context, the SIDC research group received at the 12th European Space Weather Week the “International Marcel Nicolet medal 2015” for structuring the international space weather community. EIT images as an icon of the Sun in popular press.

EIT, together with the LASCO

Over the years, EIT images made it to popular science and eventually appeared as an illustration in the worldwide press whenever the Sun was mentioned.



Figure 17: EIT images as an icon of the Sun in popular press.

The STCE Annual Meeting

The STCE Annual meeting 2015 took place on 11 June. After a brief introduction by Ronald, a fully packed Meridian room first enjoyed a presentation on SOLSPEC by David Bolsée after which Simon Chabrilat gave a summary on the workshop "Natural Hazards assessment for Aviation" (see the [5 June 2015](#) STCE Newsletter, and pp. 34 of this annual report).

Then started the main part of the meeting, i.e. the visit of various important but not-so-well-known labs and tools which are spread all over the Space Pole. For this "Points-of-Interest" tour, the participants were split into small groups of about 5 persons. Each group was accompanied by a guide who knew his/her way around the Pole. The visit of each



Figure 18: Koen Stegen explaining the secrets of the SDO Data center.

point took only 10 minutes or less, making this a quite dynamical and very interactive walk.

Visits included the high-tech Detector Lab (Samuel Gissot and Boris Giordanengo), SDO Data center (Koen Stegen) which handles 1.5 Terabytes (!) per day, and the meteo measurements and satellite techniques lab showing amongst other the cubesats (Andre Chevalier and Christian Conscience).



Figure 19: Michel Kruglanski explaining the operations of the B.USOC.

The visit to the Electronics Lab and Engineering Realizations (Eddy Neefs and Sophie Berkenbosch) gave the participants a good idea on the fine art of soldering. Michel Kruglanski showed the very operational nerve centre B.USOC (Belgian User Support and Operations Centre), and provided a

practical example with the FSL (Fluid Science Laboratory) which is aboard the ISS but controlled and operated from the B.USOC.



Figure 20: A view on the Clean Room in the BISA's basement.

The tour continued with a visit of the very Clean Room (Eddy Equeter), and participants also enjoyed an impressive performance of the 3D printer and machinery (Jeroen Maes).

There was also a tour stop at the big meteor antenna (Hervé Lamy) in the meteo park, as well as at the Solar Mechanics and Electronics lab and the Solar Dome (Jean-Luc Dufond, Aydin Ergen and

Ghislain Rigo). The sunny weather provided also an opportunity for sunspot observing.

One more point-of-interest remained, and that was the canteen of the RMI where food and refreshments were served and much appreciated. It concluded a great edition of the STCE Annual meeting.



Figure 21: Recovering from the "Points-of-Interest" tour in the RMI canteen.

Fundamental Research

The sunspot number's new clothes

The Sunspot Number, the longest scientific experiment still ongoing, is a crucial tool used to study the solar dynamo, as well as space weather and climate change. In 2011, the [WDC-SILSO](#), together with a community of about 50 scientists, initiated the first end-to-end recalibration of this reference data set. In July 2015, a first updated version of the series was officially released. Several major improvements concerned the “modern” part of the series, from 1850 to the present.

Sunspot Number research could be compared to a marathon in the sense that thanks to curious scientists such as Galileo, we have observational sunspot data dating back to 400 years ago. But, while the amount of



Figure 22: Sunspot drawings made by J.C. Staudacher on 13 and 15 February 1760.

data is impressive, the accuracy of the observations from 400 years ago differs from that of today. For example, what was sometimes seen as only one group of spots at the time (Figure 22), would in fact be counted as several groups nowadays. This difference can drastically impact the Sunspot Number

(composed of both the number of groups and the number of spots on the Sun) extracted from these particular data series.

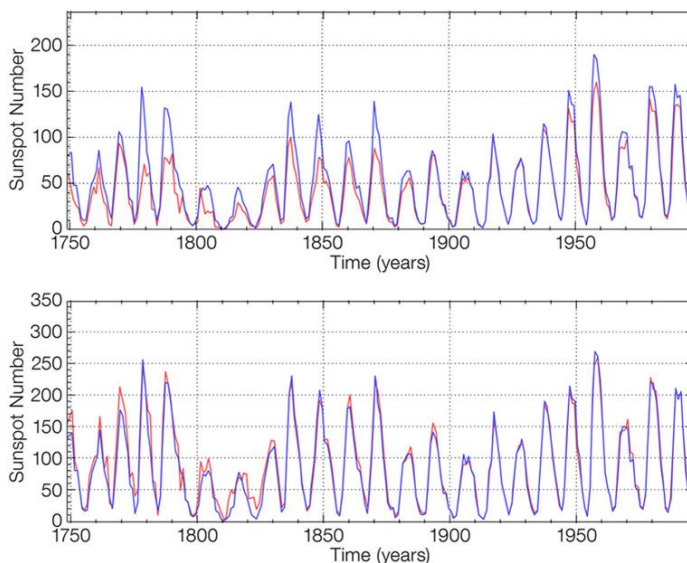


Figure 23: Sunspot Number (blue) and Group Number (red) before the corrections (upper panel) and after corrections (lower panel). Agreement between these two well-known series is improved after corrections.

Sunspots are an important scientific tool for the study of the Sun all the way to the climate on Earth. However, these accuracy problems caused by a lack of knowledge at that time or documentation afterwards, have to be taken into account.

This is why a team of scientists, including Drs. Clette and Lefèvre from the WDC-SILSO, took it upon themselves to correct and improve the data. To identify possible issues, two official sunspot series were taken into account: the International Sunspot Number (the blue line in the graph of Figure 23) and the Group Sunspot

Number (red). The results of the two lists are largely similar, but occasionally there are noticeable inconsistencies in the numbers (upper panel of Figure 23).

The corrections found change the long-term history of solar activity: what we call the “Modern Maximum” (a very active period that starts around the 1950’s) is not so different from the rest of the sunspot series anymore (lower panel of Figure 23). This fact is important for the analysis of the evolution of the Earth’s climate. Indeed, the tendency for solar cycles to be higher and higher as we progress towards the present almost vanishes after correction.

The results of this important solar community effort were announced in August 2015 at the [General Assembly of the International Astronomical Union](#).

Time variability of Integrated Water Vapour content

Since water vapour is the most dominant greenhouse gas, the presence of water vapour in the atmosphere gives rise to a doubling of the global warming that would occur in its absence (Dessler and Sherwood, 2009). It is therefore crucial to investigate and understand the time variability of the total water vapour amount in the atmosphere, both in observations and in climate model output. Therefore, for more than 100 Global Positioning Satellite (GPS) stations worldwide permanently observing since 1995/1996, we extracted the Integrated Water Vapour content (IWV) from the measured Zenith tropospheric Total Delays (ZTDs), by making use of additional meteorological data (surface pressure, surface temperature, weighted mean temperature) at the site location. A sensitivity test of the impact of these meteorological data from different sources (i.e. using two different numerical weather model outputs, and synoptic observations) on the derived IWV values and trends has been undertaken. We found that the GPS IWV trends are not too strongly affected by the used meteorological dataset, because the trends are really in the ZTD data. Another important finding is that the surface pressure has

the largest impact within the conversion procedure.

Then, we compare the IWV trend estimates (see Figure 24) – based on monthly anomalies – with trends calculated from the merged satellite GOME/SCIAMACHY/GOME -2 (hereafter: GOMESCIA) IWV retrievals at the locations of the GNSS stations. In addition, the GPS-based and GOMESCIA-based trend estimates are confronted with an external reference: trends

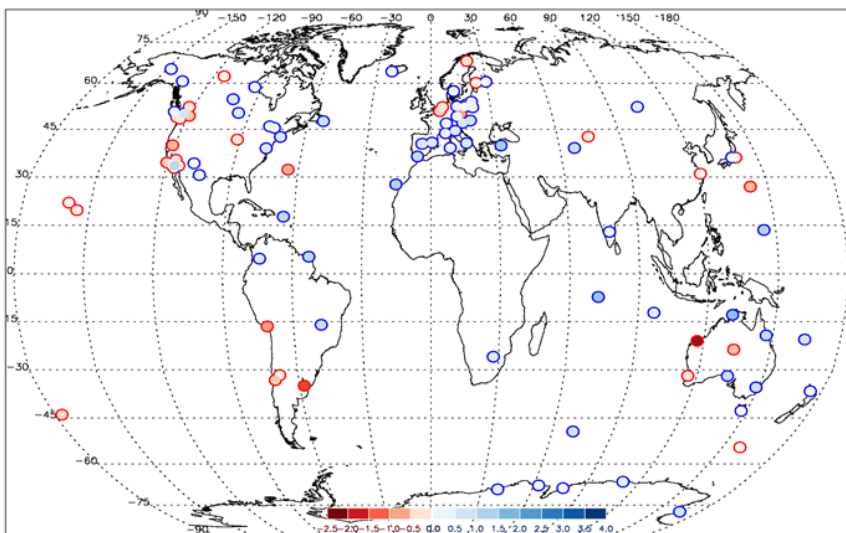


Figure 24: Trends (in mm/decade) in Integrated Water Vapour calculated from the about 100 GPS sites with data starting in 1995/1996 and with a homogeneous data processing from this date to March 2011. The trends are therefore calculated for the period 1997 to March 2011.

calculated based on a reanalysis ([ERA-interim](#)) by a numerical model of the European Centre for Medium-Range Weather Forecasts. Apart from some geographical inconsistencies in the trends for all the datasets (see Figure 24 for the GPS-based dataset), a good agreement between the GPS and ERA-interim IWV trends was found (a correlation coefficient of 0.64), and a worse agreement between GPS and GOMESCIA IWV trends (in this case, the correlation coefficient is only 0.40). The observation time separation between the GOMESCIA overpass times and the used GPS observations (at 0h and 12h UTC) only marginally affects the worse agreement in trends, so the impact of the clear sky bias of GOMESCIA retrievals on the trends might be more important. In all cases, the three different datasets give a very similar IWV seasonal cycle at the considered sites.

Finally, we investigated the applicability of the Clausius–Clapeyron equation on our datasets. This is a simple thermodynamic law stating that the water holding capacity of the atmosphere increases with a rate of 7% per 1°C temperature increase. Therefore, in Figure 25, the IWV trends (in %/decade) of the GPS dataset are considered with respect to the surface

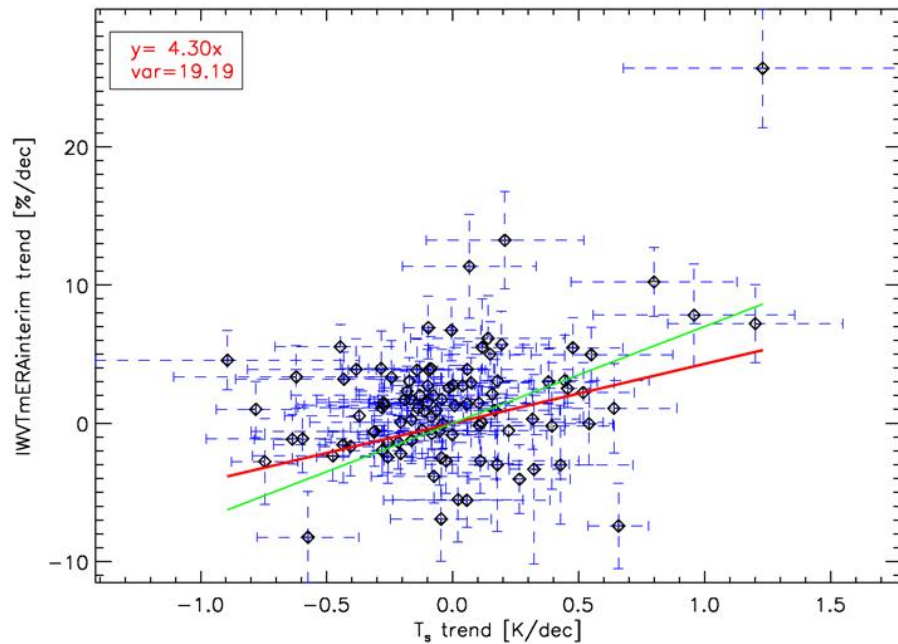


Figure 25: Diagram showing the trends (in %/decade) in Integrated Water Vapour calculated from more than 100 GPS sites (see Figure 24) with respect to the surface temperature trends at the same sites, calculated from ERA-interim. The green curve shows the Clausius–Clapeyron relation, the red curve is the linear regression calculated from the trends. The 1 sigma trend uncertainties are also shown.

temperature trends at the 100 sites. The Clausius–Clapeyron relationship is visualized by the green curve (a linear regression with a slope of 7). The linear regression calculated from the estimated trends (shown in red in Figure 25) has however a slope of only 4.3. Apart from expected local breakdowns of this relationship, homogeneity issues (no correction for breaks in the IWV time series due to e.g. antenna/sensor changes) affecting the trends in both the temperature and the IWV time series need to be taken into account. In this context, we took the lead of a homogenization activity within the European COST action GNSS4SWEC (“Advanced Global Navigation Satellite Systems tropospheric products for monitoring severe weather events and climate”).

Plasma turbulence and ion beams in the solar wind

The solar wind is a plasma: It consists of charged particles (mostly electrons and protons) forming a kind of gas, but with a density that is so low that these particles hardly collide with each other. They do

interact, however, via the electric and magnetic fields that are present in the solar wind. Especially the interplanetary magnetic field (IMF), the outward extension of the magnetic field in the solar atmosphere, creates structures in the solar wind plasma.

The solar wind is very dynamic. The electric and magnetic fields exhibit turbulent fluctuations, which can be regarded as a combination of waves. Since many years it is known that Alfvén waves are omnipresent in the solar wind. These are waves in the plasma that correspond to oscillating motions of the magnetic field and of the plasma particles transverse to the IMF direction (similar to the oscillating motion of a guitar string). The properties of these waves have been studied mostly for long wavelengths (large spatial scales), in which case one speaks of magneto-hydrodynamic (MHD) Alfvén waves. Such waves only involve fluctuating electric fields perpendicular to the magnetic field, not parallel to it. Attention has turned recently to a variant of these waves for short wavelengths (small spatial scales), the so-called kinetic Alfvén waves (KAWs). In this case, there are fluctuating electric fields parallel to the magnetic field. This is important because parallel electric fields can accelerate particles, i.e. give them more energy.

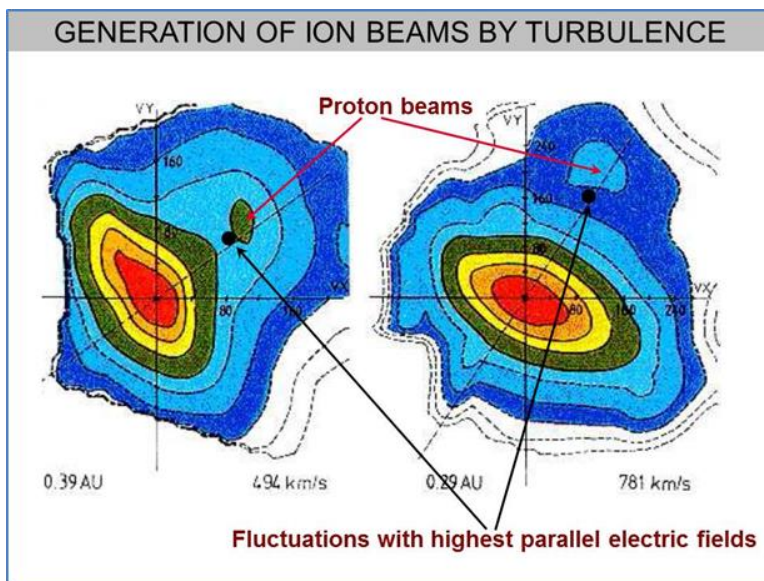


Figure 26: The distributions of the velocities of the solar wind protons in a plane containing the magnetic field direction (represented by the tilted line) for two positions in the solar wind (left: “slow” solar wind with bulk speed of 494 km/s, at 0.39 times the Earth’s distance from the Sun; right: “fast” solar wind with speed 781 km/s, at 0.29 times the Earth’s distance from the Sun). Each distribution has a marked peak, corresponding to the bulk of the solar wind protons, but there is also a secondary peak, shifted along the magnetic field direction, representing particles with higher velocities; this is the accelerated proton beam.

In an ordinary fluid, say, a cup of coffee with milk, one can add energy at large scales by stirring the coffee with a spoon, creating vortex motion. As large-scale vortices interact with each other, they create smaller vortices, down to ever smaller spatial scales, effectively mixing the milk in your coffee. The energy is carried from large vortices over smaller vortices down to the molecular level, where the molecules that make up your coffee collide, converting the energy into heat. This process is called the “energy cascade” and is at the heart of turbulence theory. It is used daily to make combustion engines run smoother, to reduce aerodynamic drag around a car, to minimize noise production by airplanes, etc. A similar kind of turbulent behaviour is found in the solar wind. Dynamic events in the solar corona provide energy input on large scales (on

the order of 1.000.000 km) into the solar wind plasma. This creates vortices, fluctuations, waves, at ever smaller scales. The turbulent fluctuations appear to be mostly Alfvén waves. Eventually, at small scales corresponding to the ion gyroradius (the radius with which the solar wind protons circle around the IMF magnetic field lines, about 100 km at the Earth’s distance from the Sun), these Alfvénic fluctuations are no longer of the MHD type, but become KAWs.

We have shown that a turbulent ensemble of these KAWs can increase the energy (and thus the velocity) of a part of the protons in a very specific way: they generate proton beams along the IMF direction. The basic process leading to such beam formation is the reflection of protons off the turbulent fluctuations (by interacting with the parallel electric field in the waves), and this happens exactly at the ion gyroradius scale. An example of such beams – which have actually been observed by spacecraft – is given in Figure 26.

This figure shows, at two positions in the solar wind (left: “slow” solar wind with bulk speed of 494 km/s, at 0.39 times the Earth’s distance from the Sun; right: “fast” solar wind with speed 781 km/s, at 0.29 times the Earth’s distance from the Sun), what the distributions of the velocities of the solar wind protons in a plane containing the magnetic field direction look like (the field direction is represented by the tilted line). One sees that the distribution has a marked peak, corresponding to the bulk of the solar wind protons. However, there is also a secondary peak, shifted along the magnetic field direction, representing particles with higher velocities. This is the accelerated proton beam mentioned before. For the typical intensity of the turbulent fluctuations observed in the solar wind, our theory predicts beam number densities of about 10% of the total solar wind density, and beam velocities of about 1.3 times the propagation velocity of Alfvén waves. These values fit the beam parameters measured in the solar wind well. In general, more energetic proton beams with higher densities and velocities are generated in environments with higher turbulence levels and/or a hotter proton background. These trends are to be examined by future solar wind observations, for instance by Solar Orbiter.



Figure 27: Who would have thought that Cappuccino got to do something with magneto-hydrodynamics (see text above)? It may provide a clue in explaining the tremendous success of the newly installed coffee machine at the ROB, with more than 30.000 servings during its first year of operation alone!

Instrumentation and experiments

Pilot Network for Identification of TIDs in Europe

Work on a new international project “Pilot Network for Identification of Travelling Ionospheric Disturbances in Europe” (Net-TIDE) started in 2015. Net-TIDE is funded by the NATO [Science for Peace and Security Programme](#) which provides a platform for governmental and scientific organizations to address emerging security threats by bringing together all available resources including scientific expertise.

The main objective of the Net-TIDE project is the establishment of a pan-European network of digital ionosondes in order to identify and estimate (travelling) ionospheric disturbances (TIDs) that can adversely affect radio communications and navigation. The project aims at developing a prototype system that provides, in real-time, an assimilative electron density model of the ionosphere with the required sensitivity to identify and track Travelling Ionospheric Disturbances (TIDs). The system will make use of the existing network of DPS-4D digital ionospheric sounders in Europe which will be trained to diagnose the TIDs applying the Frequency and Angular Sounding (FAS) technique. The FAS technique is based on measuring the variations of the angles-of-arrival and Doppler frequencies of ionospherically-reflected high-frequency (HF) radio signals. It offers a possibility of using transmissions from broadcasting stations as probing signals, leading to reduced overall system costs by using a single receiving site to monitor several transmitters making measurements over a large area.

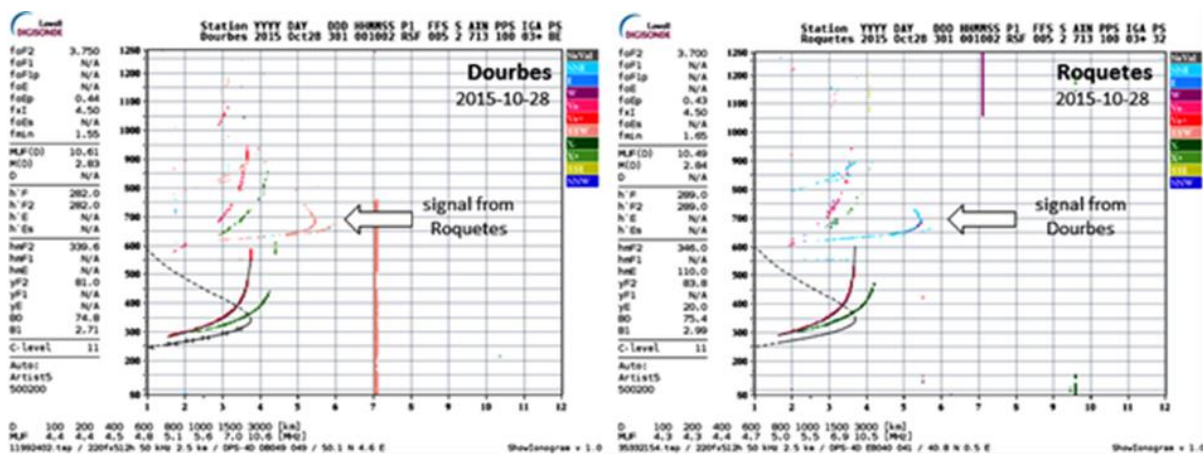


Figure 28: Synchronous ionogramming (VI+OI) with reception of both vertical and oblique echoes - digital ionograms from the observatories in Dourbes, Belgium (left) and Roquetes, Spain (right) produced on 28 October 2015 at 00:10UT. The signal coming from the other (partner) station is clearly seen on each ionogram.

Another objective is the implementation, for the first time, of a novel experimental technique for identification and tracking TIDs over a specific region, such as Europe, using high precision ionospheric DPS-4D sounders operated by the participating nations. The performance of this technique is expected to be much more reliable than other (indirect) methods since it is based on direct observations, which is one of the novel aspects of the project.

All this will lead to the development of a robust, effective, and relatively inexpensive system for remote detection and diagnostics of ionospheric irregularities that can provide information and warnings directly exploitable by the users in support of their developments of mitigation techniques.

During the first phase of the project, the network between the participating Digisondes has been set up, including developing the software for processing the (raw) observation data and computing the basic parameters that specify the bistatic links. Consequently, the Digisonde operators were able to perform all necessary adjustments and upgrades to satisfy the requirements of the Net-TIDE operational sounding modes:

- Digisonde-to-Digisonde (D2D) Skymapping. This is a 40-sec fixed-frequency transmission with 4-channel spectral data, collected at the highest possible schedule cadence (optimal, 2 - 5 minutes). In this mode, one Digisonde is set to transmit and the other one is in a radio-silent reception mode. D2D skymapping is the main source of data needed for the FAS calculations of TID parameters.
- Synchronous ionogramming (VI+OI) with reception of both vertical and oblique echoes. If Digisondes operate with identical ionogram programs, they are able to collect not only their own vertical incidence (VI) signal but also the oblique incidence (OI) signal from the partner station (cfr. Figure 28). Oblique ionograms are to be used primarily for studying the anomalous signatures of propagation caused by TIDs.
- Dedicated oblique incidence (OI) ionogram mode. This is ionogramming with one station transmitting and the other one in a radio-silent reception mode. The dedicated (OI) mode is similar to the synchronous (VI+OI) ionogramming mode but the (OI) ionogram has to be scheduled in addition to the regular vertical (VI) mode but allows for longer radio paths to be involved. Oblique ionograms from this mode will be used mainly for studies of special (ionospheric) signatures.
- Transmitters-of-Opportunity Reception (TOR). The TOR-mode is based on the capability of the Digisonde to receive and process signals from high-frequency (HF) transmitters. This is a 40-sec fixed-frequency reception with 4-channel time-domain data, collected at the highest possible schedule cadence (optimal, 2 - 5 minutes). Various HF transmitters in Europe can be used for the purpose.

In parallel with the setup of the operational network of Digisondes, a database system was designed and developed for the raw data files received by the Digisondes. The Lowell ObliquE Incidence database (LOUI-Base) is a suite of databases holding data from oblique sounding of ionosphere with digisondes, as well as accompanying software tools for data ingestion, processing, modeling, detection and evaluation of the TIDs.

The Net-TIDE Digisonde network and the related database are now fully operational, with first measurements and scientific results already [available](#) to partners and registered users.

Thanks to the continuous efforts of the scientific personnel during the years and investments in state-of-art equipment, combined with long-time provision of various high-quality measurements and services, RMI was invited to join this international project with the ionospheric sounder in Dourbes selected as the project's reference station. The NATO funding allows for further investments in the Dourbes observatory and for the researchers to further improve expertise, products, services, and cooperation.

Ionosonde observations of the 20 March 2015 solar eclipse

During the morning hours of 20 March 2015, a total solar eclipse occurred over the Northern part of the Atlantic Ocean (Figure 29). Though Belgium was not in the path of eclipse totality, it experienced a partial solar eclipse with a maximum obscuration of 81.5% reached at 09:34UT. This is already a very significant eclipse, observable not only in visible light but also in the ionizing radiation responsible for producing the plasma that makes up the ionosphere.

At the RMI Geophysical Research Centre in Dourbes, an advanced digital sounder, Digisonde-4D, is continuously monitoring the ionosphere in [real-time](#). It is used to study not only the local vertical distribution of the plasma density but also the plasma gradients and transport in the vicinity of the observatory. In its usual, real-time operational mode, the ionosonde makes measurements at 5-min intervals. In order to study the quick reaction of the ionosphere in response to the eclipse, it was decided to run an unprecedented campaign of measurements with a 30-seconds time resolution.

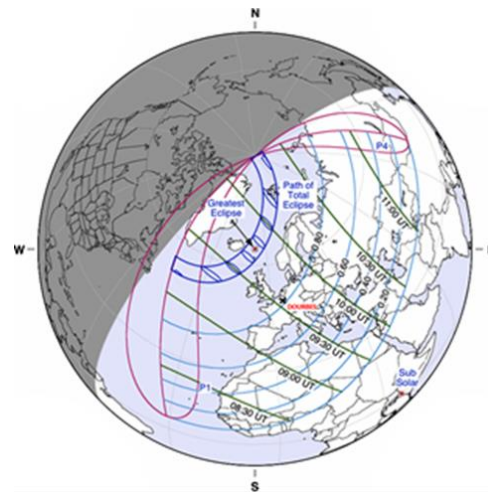


Figure 29: Path of the solar eclipse on 20 March 2015 (credit: [NASA](#)).

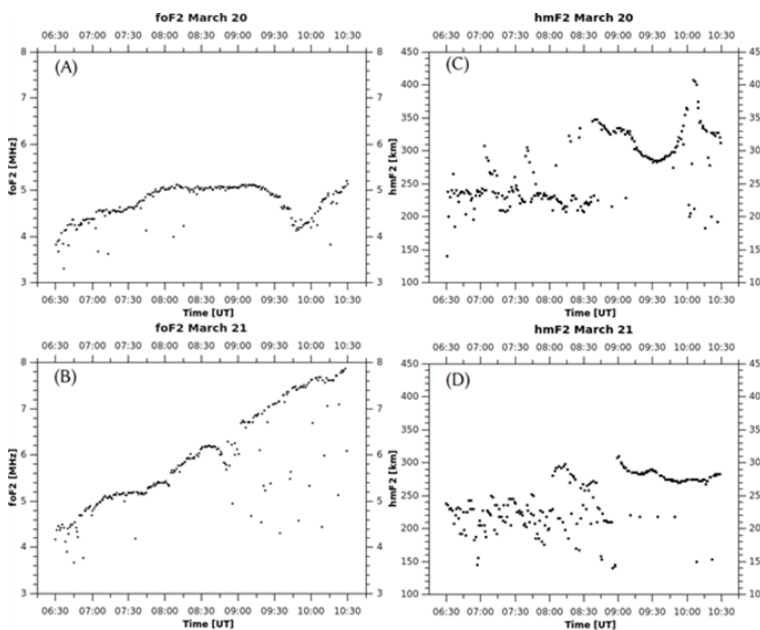


Figure 30: The ionospheric critical frequency (left) and ionospheric peak-density height (right) of the ionospheric electron density as measured by the Dourbes digital ionosonde. The top panels show the data from March 20, the day of the solar eclipse. The bottom panels show the same characteristics measured on March 21, showing the typical morning-time behaviour for this season.

The high-resolution observations yielded excellent results (Figure 30) for the ionospheric critical frequency foF2 (equivalent to the ionospheric peak density NmF2) and the ionospheric peak-density height (hmF2) during the eclipse. For a better analysis, the bottom panels (B) and (D) show the same observations during a “normal” day, the one after the eclipse. In panel (B), the normal evolution of the peak density during sunrise can be seen: under the influence of the increasing ionizing radiation, the density of electrons gradually increases from its night-time value to its day-time equilibrium. Panel (A) shows the same parameter during the eclipse. The eclipse starts at 08:27UT, and ends at 10:47UT. It is clear that during the eclipse the production of ionization

is halted and, near the maximum obscuration, the peak density even goes down - together with a sudden upswing in the height of the peak (panel C). This is the behaviour that normally happens at sunset, and this eclipse provides a unique opportunity to study the non-equilibrium conditions that normally only happen around transitional periods of sunrise and sunset.

One interesting observation made during the eclipse, for example, is that the deviation in the peak density starts before the onset of the eclipse at the location of the ionosonde. This demonstrates the importance of taking into account the transport of plasma, in addition to the local ionization and recombination equilibrium.

Total Solar Irradiance

On 2 December 2015, we celebrated the 20th anniversary of the launch of our DIARAD/VIRGO instrument on the SOHO satellite. After 2 decades, DIARAD/VIRGO is still operational providing a measurement of the Total Solar Irradiance (TSI) every 3 minutes. The DIARAD/VIRGO instrument has been developed by the Royal Meteorological Institute of Belgium and the Belgian company Verhaert NV, which has now become Qinetiq Space.



Figure 31: Celebration of 20 years of DIARAD/VIRGO in space.

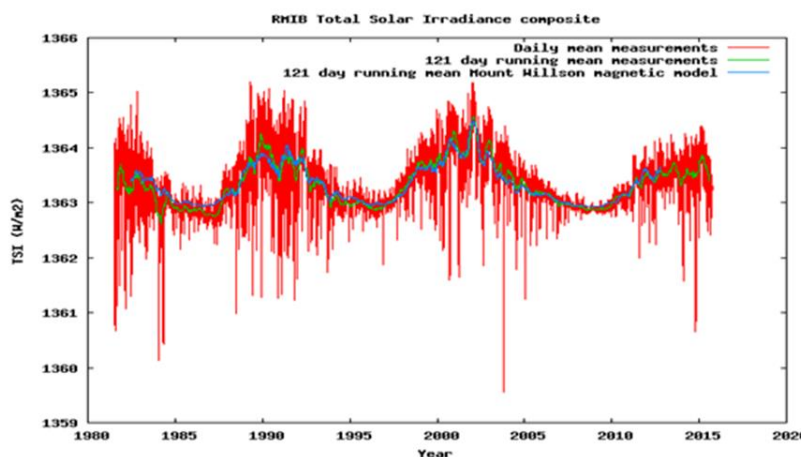


Figure 32: The RMIB Total Solar Irradiance composite.

The measurements of DIARAD/VIRGO are important for the quantification of the possible influence of the Sun on climate change on the Earth. They are used in the [RMIB TSI composite](#) which is internationally recognized and is used by the NASA Ceres project for the monitoring of the Earth radiation net imbalance.

We now dispose of reliable TSI space measurements over 3 minima of the 11 year solar cycle, showing no significant change of the TSI level in between the solar minima. From the longer ground based sunspot observations, for which a revised time-series was

published by the Royal Observatory of Belgium in July 2015 (see pp. 18), we know that the 11 year solar cycle amplitude is modulated with roughly a 100 year periodicity and that currently we are near the minimum of this 100 year modulation. From these combined space and ground observations we can draw the important conclusion that the Sun did not have a significant impact on climate change on Earth over the last 300 years.

The results of the laboratory measurement campaign that we conducted in 2013 indicate that the new value of the “Solar Constant” of 1361 W/m^2 proposed by the TIM/SORCE team is too low. Our best estimate of 1363 W/m^2 was presented at the SORCE Sun-Climate Symposium in November 2015.



Figure 33: International Pyrheliometric Comparison at PMOD in Davos.

We have been invited to provide a TSI instrument for the Chinese operational meteorological polar satellite FY3E with launch currently scheduled for 2018. The satellite will fly an early morning dusk/dawn orbit and will have a design lifetime of 8 years. It is the first time that the China Meteorology Agency (CMA) – comparable to Eumetsat in Europe – invites non-Chinese partners (RMIB in Belgium and PMOD in Switzerland) to provide an instrument for flight on an operational meteorological satellite. This gives us the ideal opportunity to continue our very successful DIARAD/VIRGO measurements, and it allows entering into a strategic collaboration with CMA, not only in the field of TSI measurement but also in the field of the Earth Radiation Budget (ERB)

measurement. We received a delegation from CMA and CIOMP to kick off the project in October 2015. The design of our new TSI instrument, called SOLar VARIability Monitor (SOLVAM) has started.

We participated in the [International Pyrheliometric Comparison](#) (IPC) 2015 which was held in Davos. The aim of these gatherings, which take place every 5 years at the WRC in Davos, is to ensure the worldwide transfer of the [World Radiometric Reference](#). During this event, all participants bring their instruments, solar-tracking and data acquisition systems to Davos to conduct simultaneous solar radiation measurements with the World Standard Group.

PICASSO-SLP, a space weather instrument for a scientific nano-satellite

PICASSO is a CubeSat ESA mission initiated by BIRA-IASB. One of its payloads is SLP, the Sweeping Langmuir Probe, which has been developed in-house. The STCE has contributed significantly to this instrument. As required for CubeSat payloads, SLP has a small volume, a small mass, a small power consumption,... but potentially great science: it will measure the plasma density and temperature in the upper ionosphere.

The launch of PICASSO is foreseen for the spring of 2017. Apart from SLP, it also carries a miniaturized imaging spectrometer (VISION). It will fly for 2 years along a polar orbit at about 500 km altitude. The

orbital period is about 90 minutes. The platform is a triple-unit CubeSat (10x10x32 cm; 3.7 kg), equipped with 4 deployable solar panels. UHF/VHF radio is used for the satellite telemetry/telecommand and S-Band for the scientific telemetry, with up to 50 MB of scientific data downlink per day. In order to satisfy the pointing requirements of VISION and of the S-Band antenna, the CubeSat relies on 3 reaction wheels in addition to magnetorquers. The platform, the payload integration and the operations are carried out by Clyde-Space (UK).

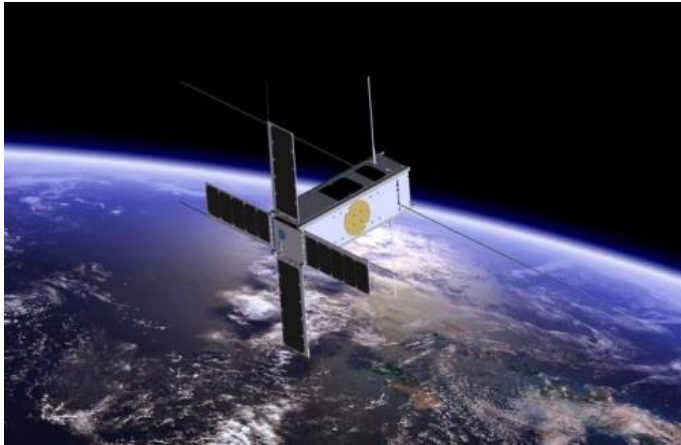


Figure 34: The PICOSatellite for Atmospheric and Space Science Observations (Picasso) CubeSat is designed to investigate the upper layers of Earth's atmosphere.

The operating principle of a Langmuir probe is straightforward. Assume that the external surface of the spacecraft represents the electrical ground. A Langmuir probe then is an electrically conducting surface that is placed at some distance away from the spacecraft. One imposes a potential difference between the probe and the spacecraft, and one measures the current collected or emitted by the probe. One sweeps over a range of potentials (typically between -5 V and +15 V) in order to determine the current-voltage characteristic. From this curve, one can determine the electron density, electron temperature, as well as the spacecraft potential.

The challenges for SLP are the following:

- Provide probes (in this case, 4 needle probes) sufficiently far away from the spacecraft body: this is done by mounting the probes at the extremities of the solar panels.
- Remain within the volume/mass/power constraints.
- Measure the tiny currents with sufficient accuracy, especially by trying to reduce the noise.
- Avoid satellite charging while the probes are collecting current, due to the small total outer surface area of the spacecraft.

In 2015 the SLP design was essentially completed; for 2016 the actual construction of the instrument is on the table.

SLP promises to be an interesting instrument for space weather purposes. Every 90 minutes, PICASSO will pass through the ionosphere above each polar cap, providing measurements on the topology of the magnetosphere as the size of the polar cap offers information about the role of ongoing magnetospheric reconnection. Near the auroral oval, we expect to see the signature of aurora, including plasma cavities in the upper ionosphere. Above the lower latitude zones, SLP is essentially measuring the interface between ionosphere and plasmasphere. All of this fits in with the research themes currently addressed at BIRA-IASB and has space weather relevance.



Figure 35: This picture of the aurora was taken by Birgit Ritter, and subsequently processed by Luciano Rodriguez. The picture was taken from Kiruna (Sweden) on 15 October 2015.

Applications, Modeling and Services

Automatic detection of CMEs in Heliospheric Imager data

The advent of wide-angle imaging of the inner heliosphere has revolutionized the study of the solar wind and, in particular, solar wind structures such as Coronal Mass Ejections (CMEs). CMEs comprise enormous plasma and magnetic field structures that are ejected from the Sun and propagate at what can be immense speeds through interplanetary space. With Heliospheric Imaging (HI) came the unique ability to track the evolution of these features as they propagate through the inner heliosphere. Prior to the development of wide-angle imaging of the inner heliosphere, signatures of such solar wind transients could only be observed within a few solar radii of the Sun, and in the vicinity of a few near-Earth and interplanetary in-situ probes. HI has, for the first time, filled that vast and crucial observational gap, as can be seen in Figure 36.

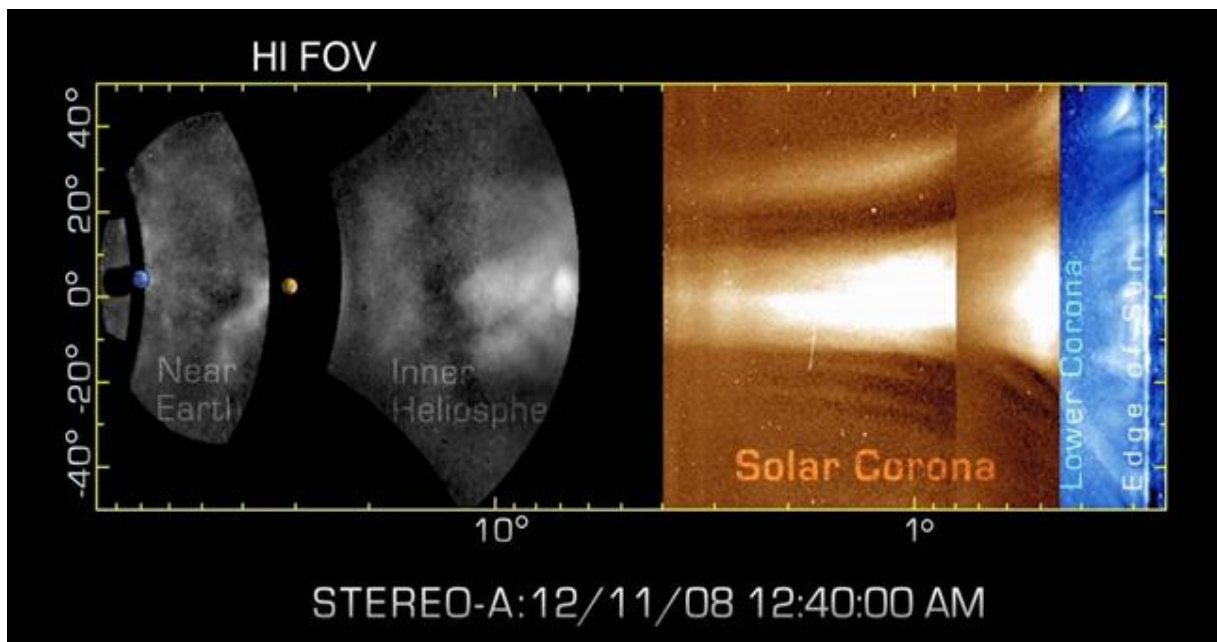


Figure 36: Combined view of coronagraphs (blue and yellow) and heliospheric imagers (grey) showing the solar wind and CMEs between the Sun and the Earth. The Sun is at the right of the image, the Earth is at the left. See [Howard et al. \(2012\)](#), and the associated [press release](#).

The European FP7 [HELCASTS](#) project provides access to advanced catalogues - validated and augmented through the use of techniques and models - for the analysis of solar wind structures, based on observations from European-led space instrumentation, providing a strong foundation for enhanced exploitation and advancement of European heliospheric research.

ROB's task consisted of the implementation of a technique to automatically detect CMEs in HI data. Therefore, we have adapted [CACTus](#) to work with HI images as it was only working with coronagraph data up to that point (SOHO/LASCO and STEREO/COR2). This was a big challenge due to several factors. The geometry of the observations is completely different, CMEs are fainter in HI data, the images include planets and stars that have to be removed, and the cadence is much lower than that in a regular coronagraph.

In spite of all the complications, we have succeeded to modify CACTus to work with HI. It is the first time that this task has been performed successfully. The result of this work is the production of a catalogue of automatically detected CMEs in HI data for the full duration of the STEREO mission (from 2007 until present). This catalogue contains about 1000 CMEs, and it is available at the website of the [SIDC](#). A snapshot of the catalogue is shown in Figure 37. A real-time output will be available in the near future.

A comparison of our automatic CME catalogue with a pre-existing manually-made CME catalogue is underway. This exercise, apart from providing validation to our method, is allowing us to obtain important insights on the automatic algorithm itself, and providing important constraints and

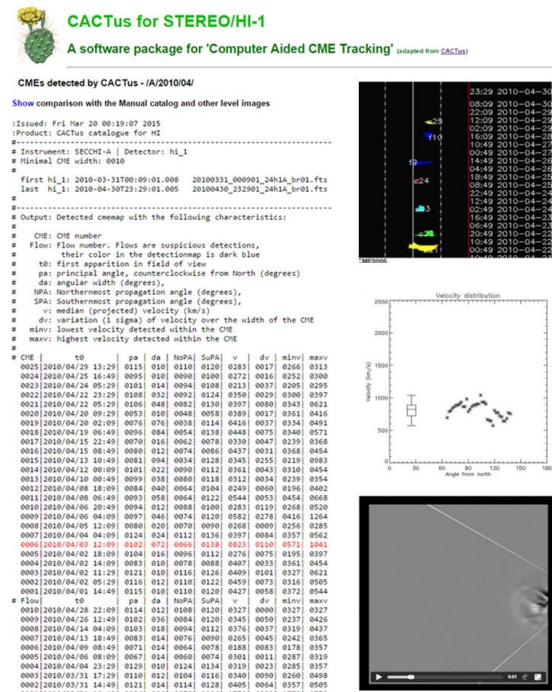


Figure 37: The HELCATs automatic CME catalogue. The events are listed on the left, and when clicking on them information on the CME is obtained (a video on the bottom right and information on the CME speed on the middle right).

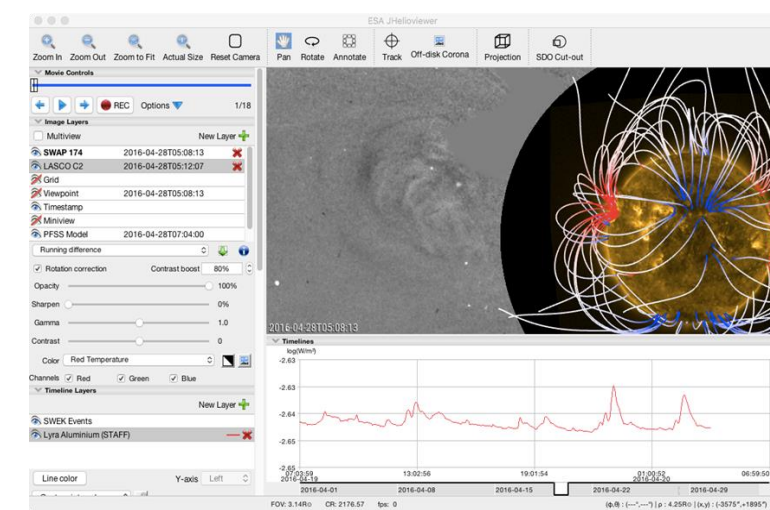


Figure 38: Screenshot of a jHelioviewer session showing a PROBA2/SWAP image (yellow) with a magnetic field extrapolation (PFSS, red-white-blue) and in the background a SOHO/LASCO C2 difference image showing a CME. The bottom panel shows a PROBA2/LYRA timeline with flares.

information that can be applied to enhance our knowledge on CMEs.

Sunny views with jHelioviewer

The activity on the Sun is monitored by many different solar telescopes both on the ground as well as in space. Satellites such as the NASA STEREO mission even image the backside of the Sun. In many cases, the data is available in near real-time from various websites. For a solar physicist or a space weather operator, it can become quite labor intensive to crawl through all the

available data and make a synthesis of what is going on at the Sun.

For these reasons, a team of software developers at ROB have overhauled the existing jHelioviewer application and boosted its functionalities. Once installed on the user computer, jHelioviewer allows

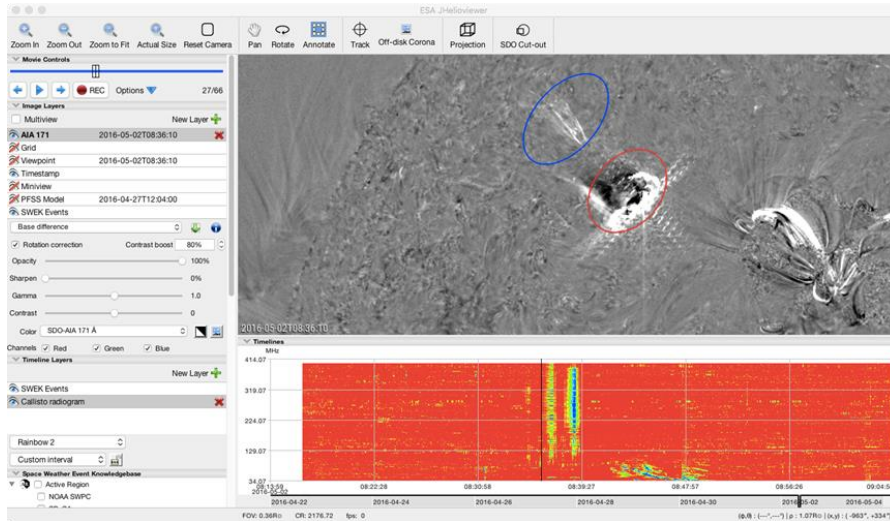


Figure 39: Screenshot of a jHelioviewer session showing an SDO/AIA difference image with an ongoing flare spray (blue circle) and flare (red circle). The bottom panel displays a Humain/eCallisto radiospectrograph showing a coinciding type II radioburst.

you to access a variety of solar data from different servers and, by just clicking a few buttons, display movies of combined data sets, with chosen zoom and perspective and even with your favorite projection. The new version also incorporates access to space weather events (e.g. flares) and displays their timelines synchronized with the running movie.

This new version 2.10 has been improved under the contract “High Performance Distributed Solar Imaging and Processing System” of the European Space Agency (ESA), awarded to the SIDC of the Royal Observatory of Belgium (ROB). The application is freely available for all platforms and [online](#), where also a user manual is available. At the time of this writing (May 2016), hundreds of users worldwide have downloaded the extremely versatile application.

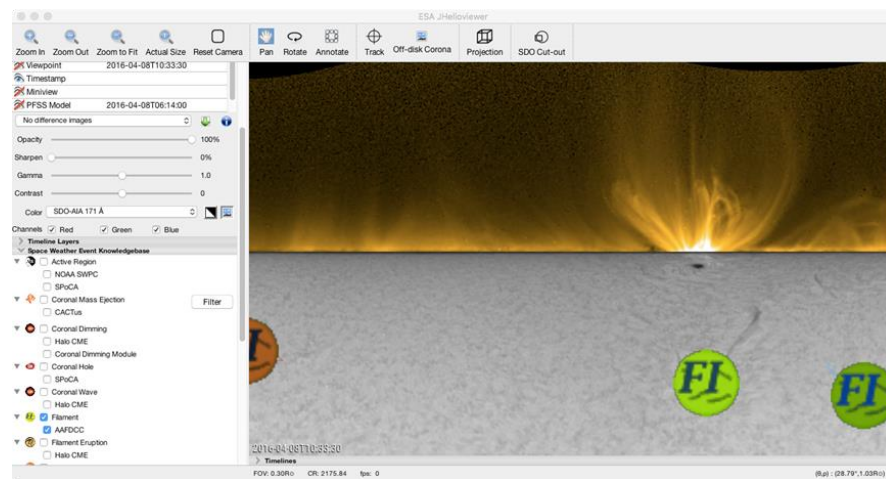


Figure 40: Screenshot of a jHelioviewer session showing a log/polar projection of a ROB/USSET H-alpha image (grey, note the sunspot) and the off-limb counterpart by PROBA2/SWAP. The “FI” labels show the location of filaments as extracted live from the [Heliosphysics Event Knowledgebase \(HEK\)](#).

PARAFOG: using ALC to forecast radiation fog

The Royal Meteorological Institute (RMI) now has an Automatic LIDAR Ceilometer (ALC) network in Belgium (Figure 41) that offers the opportunity to use the backscatter profiles (measurements by ALC) as a proxy to monitor in real-time the vertical profile of aerosols on a continuous temporal scale. An ALC is able to monitor aerosol plumes such as volcanic ash clouds which might be a hazard for air traffic. An ALC is also able to help with the prediction of radiation fog formation which is one of the most common and persistent weather hazards encountered in aviation and to nearly all forms of surface transport. Radiation fog is formed by the cooling of land after sunset by thermal radiation of the Earth in calm conditions with clear sky and in presence of hygroscopic aerosols. When this occurs at busy airports, air traffic can be significantly disrupted because low visibility at the ground makes it unsafe to take off and land.

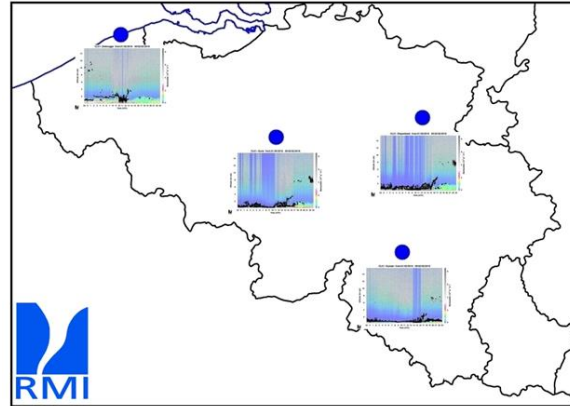


Figure 41: Map of Belgium with the locations of the ALCs in Zeebrugge, Uccle, Diepenbeek and Humain.

In the first atmospheric layers close to the ground, the backscatter profile potentially contains major information to predict if radiation fog will be formed or not. During the preliminary stage of fog formation, the backscatter profile may be influenced by atmospheric humidity due to the presence in the atmosphere of hygroscopic aerosols that see their size increase with their moisture content, inducing an increase of the backscatter magnitude. The hygroscopic growth process can occur at the surface or aloft. Hence it is important to be able to track this process over a sufficiently deep vertical profile to capture activation where it occurs first.

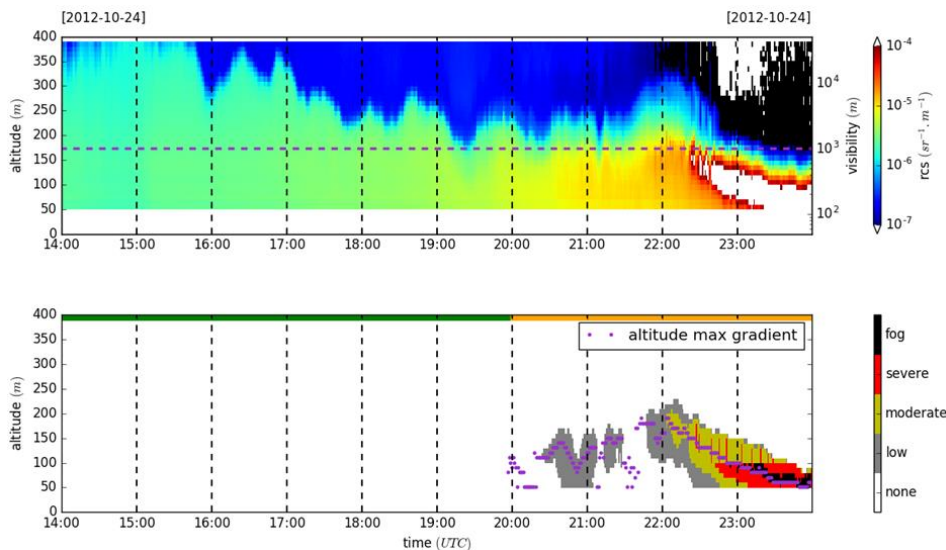


Figure 42: Time series presenting ALC measurements and alert fog levels (low, moderate, severe and fog) in pre-fog conditions on 24 October 2012 at Uccle. (a) ALC attenuated backscatter. (b) Alert fog levels and altitude where the aerosol hygroscopic growth is fastest.

Current numerical weather prediction forecasts are able to predict general conditions favorable for fog formation, but not the exact time or location of fog occurrence. Such models lack the vertical and spatial resolution and representation of boundary layer and microphysical processes to accurately

represent actual near-surface cooling rates, turbulent mixing, and their vertical structure in the surface layer. They typically do not represent accurately the activation processes of fog droplets that depend on the chemical nature of the aerosols, on their size distributions, and on typically very low supersaturation conditions.

In the framework of TOPROF (COST Action) activities in the ALC working group, collaboration was initiated between RMI and SIRTa (IPSL, Institut Pierre-Simon Laplace) to develop a forward stepwise screening algorithm (PARAFOG) to help the prediction of radiation fog formation, based on the hygroscopic growth function of aerosol scattering coefficient coupled with the standard surface weather observations. PARAFOG is unique and is the first meteorological tool in the world that uses ALC data to predict if fog will be formed or not. It was developed on the ALC dataset of Uccle and of SIRTa to derive fog formation predictors and to investigate the possibility to make short-term fog formation warnings for helping forecasters. An example is given in Figure 42 by a fog case study observed at Uccle.

Since November 2015, PARAFOG has been tested at the Paris Charles De Gaulle Airport (collaboration between SIRTa and Météo-France) as a decision support system for radiation fog forecasting.

Natural Hazard Assessment for Aviation

External hazards (weather phenomena, space weather, volcanic ash, etc.) may have a large impact on aviation safety and flight operations. Despite improving aircraft design to withstand these phenomena, severe external hazards must be avoided if possible. Therefore, awareness of the phenomena and possible impacts, together with timely and accurate information is crucial to every flight.



Figure 43: Michel Kruglanski and Erwin De Donder welcoming about 30 participants to the “Natural Hazard Assessment for Aviation” workshop on 2 June in the ROB’s Meridian Room.

To avoid impacts from adverse (space) weather conditions, pilots and dispatchers need access to up-to-date information and communication with organizations that can provide early warnings and specialized information on the encountered hazards.

Through the years, several services/products related to (space) weather hazards have been developed under the umbrella of the STCE (Solar-Terrestrial Centre of

Excellence), within the context of international projects and in specific ESA’s Space Situational Awareness programme for space weather. The aviation sector is an end user community common to the three institutes at the Space Pole (i.e. BIRA-IASB, RMI and ROB):

- The meteorological groups provides specific services to the aviation community in relation to forecasts and nowcasts on visibility, lightning, precipitation, fog formation, detection of nightly mass migration of birds etc.



Figure 44: Jesse Andries providing an overview of the SIDC and its space weather services.

- BIRA-IASB hosts the SACS (Support to Aviation Control Service) on-line service that is able to issue warning alerts for volcanic ash plumes that may have a strong impact on air traffic as was demonstrated during the eruption of the Eyjafjallajökull in 2013.
- Within ESA's SSA Space Weather programme, the Space Physics Division at BIRA-IASB and the Space Weather Department of ROB are the leading expert groups for respectively space radiation and solar weather. Space weather is a real concern for aviation. Solar flares and coronal mass ejections may produce high energetic solar particles that create high radiation doses at flight altitudes and increase the ionization in the upper atmosphere affecting the propagation of radio signals. Under the leadership of BIRA-IASB and in collaboration with ROB and international partners, the COMESEP alert system has been developed for radiation and geomagnetic storms based on real-time solar activity observations.



Figure 45: Listening to the end user needs is critical in developing products that can readily be integrated in their operations.

When developing services/products it is important that the delivered information is understandable for the end user and in a format that it can be readily integrated in their operations, which requires close interaction between the provider and the end user. It was an initiative of the space weather group at BIRA-IASB to organize this workshop on 2 June 2015 in the ROB's Meridian Room. Its aim was

to set up a first dialogue between the scientific experts at the Space Pole and the people from the

aviation community to explore what they need and what we can provide. In the presentation of the various services/products with their different characteristics, it was clear that some are already quite mature and corresponding to the needs of the end user, others are in a phase of development and need further tailoring. Some address quite global problems, others regional or local. Also the time of warning is very different for different phenomena.

From the presentation of the SESAR (Single European Sky ATM Research) project by Eurocontrol, it came out that next to the quality/reliability of information, the consistency between the formats in which information is delivered is very important. Standardization of information and regulations are requirements. Within this context, the question was raised if it wouldn't be better to have one common platform that covers all natural risks than to have several separate centres focused on one specific hazard. The answer to this is not obvious. It was proposed that the three institutes could jointly work as a coordinated centre for aviation applied services in close collaboration with Belgocontrol and Eurocontrol.

In view of the potential risks due to space weather it was pointed out by the aviation community that although the awareness is increasing, the overall aviation industry does not understand/recognize space weather effects or impacts on operations and that there is a need for education and training. Also the creation of a database with recorded impacts would be a challenge. It would help to investigate how useful/helpful the information provided by the service(s) was at that time.



Figure 46: At the end of the workshop, an informal discussion between the participants allowed for further fine-tuning of the services and products to the end user needs.

At the end of the workshop it was agreed that the interaction between the aviation community and the (space) weather research and service provider community is very useful and should be increased. Currently a campaign is running in collaboration with ECA (European Cockpit Association) with the aim to set up a space weather bulletin to support pilots and flight operators during severe space weather conditions. The campaign is

led by the space weather group of BIRA-IASB within the activities of the SSA Space Weather Coordination Centre (SSCC), located at the Space Pole and jointly operated by BIRA-IASB and ROB with technical support from Space Applications Services.



Figure 47: Scientists need energy. Lo and behold: the food-trucks made their appearance on the Space Pole. Coming in all sizes, and serving various kinds of exotic foods, they did what they were supposed to do: to fill the hungry ~~minds~~ stomachs.

Publications

This overview of publications consists of three lists: the peer-reviewed articles, the presentations and posters at conferences, and the public outreach talks and publications for the general public. It does not include non-refereed articles, press releases, the daily, weekly and monthly bulletins that are part of our public services, ... These data are available at the STCE-website <http://stce.be/index.php> or upon request.

Authors belonging to the STCE have been highlighted in the list of peer reviewed articles.

Peer reviewed articles

1. Aragon-Angel, A.; Hernandez-Pajares, M.; **Defraigne, P.**; **Bergeot, N.**; Prieto-Cerdeira, R.
Modelling and Assessing Ionospheric Higher Order Terms for GNSS Signals
Proceedings of ION GNSS+ 2015, pp. 3511-3524, 2015
2. Aschwanden, M.J.; Boerner, P.; Caspi, A.; McTiernan, J.M.; **Ryan, D.F.**; Warren, H.P.
Benchmark Test of Differential Emission Measure Codes and Multi-thermal Energies in Solar Active Regions
Solar Physics, 290, pp. 2733-2763, 2015
3. Aschwanden, M.J.; Boerner, P.; **Ryan, D.F.**; Caspi, A.; McTiernan, J.M.; Warren, H.P.
Global energetics of solar flares: II. Thermal Energies
The Astrophysical Journal, 802, 53, 2015
4. **BenMoussa, A.**; **Giordanengo, B.**; **Gissot, S.**; **Dammasch, I.E.**; **Dominique, M.**; **Hochedez, J.-F.**; Soltani, A.; Bourzgui, N.; Saito, T.; Schühle, U.; Gottwald, A.; Kroth, U.; Jones, A.R.
Degradation assessment of LYRA after 5 years on orbit - Technology Demonstration
Experimental Astronomy, 39, pp. 29-43, 2015
5. Carrasco, V.; **Lefèvre, L.**; Vaquero, J.M.; Gallego, M.
Equivalence relations between the Cortie and Zurich sunspot group morphological classifications
Solar Physics, 290, pp. 1445-1455, 2015
6. Chang, T.; Wu, C.C.; **Echim, M.**; **Lamy, H.**; Vogelsberger, M.; Hernquist, L.; Sijacki, D.
Complexity Phenomena and ROMA of the Earth's Magnetospheric Cusp, Hydrodynamic Turbulence, and the Cosmic Web
Pure and Applied Geophysics, 172, 7, pp. 2025-2043, 2015
7. **Clette, F.**; **Lefèvre, L.**
The new Sunspot Number: assembling all corrections
Solar Physics, submitted 2015, awaiting publication
8. **Clette, F.**; **Lefèvre, L.**; Cagnotti, M.; Cortesi, S.; Bulling, A.
The revised Brussels-Locarno Sunspot Number (1981-2015)
Solar Physics, 2016, DOI: 10.1007/s11207-016-0875-4
9. **Clette, F.**; Svalgaard, L.; Vaquero, J.M.; Cliver, E.W.
Revisiting the Sunspot Number
The Solar Activity Cycle, Space Sciences Series of ISSI, 53, ISBN 978-1-4939-2583-4, Springer Science+Business Media New York, 2015, pp. 35, DOI: 10.1007/978-1-4939-2584-1_3
10. Cliver, E.W.; **Clette, F.**; Svalgaard, L.; Vaquero, J.M.
Recalibrating the Sunspot Number (SN): The 3rd and 4th SN Workshops
Central European Astrophysical Bulletin, 39, pp. 1-19, 2015
11. **De Visscher, R.**; **Delouille, V.**; Dupont, P.; Deledalle, C.
Supervised classification of solar Features using prior information
Journal of Space Weather and Space Climate, 5, A34, 2015, DOI: 10.1051/swsc/2015033
12. Del Zanna, L.; Matteini, L.; Landi, S.; **Verdini, A.**; Velli, M.
Parametric decay of parallel and oblique Alfvén waves in the expanding solar wind
Journal of Plasma Physics, 81, pp. 3202, 2015
13. Dumbovic, M.; **Devos, A.**; Vrsnak, B.; Sudar, D.; **Rodriguez, L.**; Ruzdjak, D.; Leer, K.; Vennerstrom, S.; Veronig, A.M.; Robbrecht, E.
Geoeffectiveness of Coronal Mass Ejections in the SOHO era
Solar Physics, 290(2), pp. 579-612, 2015
14. Franci, L.; Landi, S.; Matteini, L.; **Verdini, A.**; Hellinger, P.
High-resolution hybrid simulations of kinetic plasma turbulence at proton scales
The Astrophysical Journal, 812, pp. 21, 2015
15. Franci, L.; **Verdini, A.**; Matteini, L.; Landi, S.; Hellinger, P.

Solar Wind Turbulence from MHD to Sub-ion Scales: High-resolution Hybrid Simulations
The Astrophysical Journal Letters, 804, L39, 2015

16. Guennou, C; **Rachmeler, L. A.**; **Seaton, D.B.**; Auchere, F.

Lifecycle of a large-scale polar coronal pseudostreamer/cavity system
Frontiers in Astronomy and Space Sciences, 2016, DOI: <http://dx.doi.org/10.3389/fspas.2016.00014>

17. **Gunell, H.**; Andersson, L.; **De Keyser, J.**; Mann, I.
Vlasov simulations of trapping and loss of auroral electrons
Annales Geophysicae, 33, 279–293, 2015, DOI: 10.5194/angeo-33-279-2015

18. **Gunell, H.**; Andersson, L.; **De Keyser, J.**; Mann, I.
Self-consistent electrostatic simulations of reforming double layers in the downward current region of the aurora
Annales Geophysicae, 33, 1331-1342, 2015, DOI: 10.5194/angeo-33-1331-2015

19. Hellinger, P.; Matteini, L.; Landi, S.; **Verdini, A.**; Franci, L.; Travníček, P.
Plasma Turbulence and kinetic instabilities at ion scales in the expanding solar wind
The Astrophysical Journal Letters, 811, L32, 2015

20. Inglis, Andrew; Ireland, Jack; **Dominique, M.**
Quasi-periodic pulsations in solar and stellar flares: re-evaluating their nature in the context of power-law flare Fourier spectra
The Astrophysical Journal, 798, 108, 2015, DOI: <http://dx.doi.org/10.1088/0004-637X/798/2/108>

21. Karlsson, T.; Kullen, A.; Liljeblad, E.; Brenning, N.; Nilsson, H.; **Gunell, H.**; Hamrin, M.
On the origin of magnetosheath plasmoids, and their relation to magnetosheath jets
Journal of Geophysical Research - Space Physics, 120, pp. 7390-7403, 2015, DOI: 10.1002/2015JA021487

22. Kotov, D.V.; Truhlik, V.; Richards, P.G.; **Stankov, S.M.**; Bogomaz, O.V.; Chernogor, L.F.; Domnin, I.F.
Night-time light ion transition height behaviour over the Kharkiv (50°N, 36°E) IS radar during the equinoxes of 2006–2010
Journal of Atmospheric and Solar-Terrestrial Physics, 132, 9, pp. 1-12, 2015, DOI: 10.1016/j.jastp.2015.06.004

23. **Kraaikamp, E.**; **Verbeeck, C.**
Solar Demon – an approach to detecting flares, dimmings, and EUV waves on SDO/AIA images
Journal of Space Weather and Space Climate, 5, A18, 2015, DOI: 10.1051/swsc/2015019

24. **Lamy, H.**; **Anciaux, M.**; **Ranvier, S.**; **Calders, S.**; **Gamby, E.**; **Martinez Picar, A.**; **Verbeeck, C.**
Recent advances in the BRAMS network
Proceedings of the International Meteor Conference, Mistelbach, Austria, 27-30 August 2015, Eds.: Rault, J.L.; Roggemans, P., International Meteor Organization, pp. 171-175, 2015

25. **Lefèvre, L.**; Vennerstrom, S.; Dumbovic, M.; Vrsnak, B.; Sudar, D.; Arlt, R.; **Clette, F.**; **Crosby, N.B.**
Detailed Analysis of solar data related to historical extreme geomagnetic storms: 1868-2010
Solar Physics, 2016, DOI: 10.1007/s11207-016-0892-3

26. Lilensten, J.; Bommier, V.; Barthélemy, M.; **Lamy, H.**; David, B.; Idar Moen, J.; Magnar Gullikstad, J.; Lvhaug, U.P.; Pitout, F.
The auroral red line polarisation: modelling and measurements
Journal of Space Weather and Space Climate, 5, A26, 2015.

27. Malovichko, P.; **Voitenko, Y.**; **De Keyser, J.**
Compensated-current instability of kinetic Alfvén waves
Monthly Notices of the Royal Astronomical Society, 452, pp. 4236-4246, 2015, DOI: 10.1093/mnras/stv1533

28. **Martinez Picar, A.**; **Marqué, C.**; **Anciaux, M.**; **Lamy, H.**
Directional pattern measurement of the BRAMS beacon antenna system
Proceedings of the International Meteor Conference, Mistelbach, Austria, 27-30 August 2015, Eds.: Rault, J.L.; Roggemans, P., International Meteor Organization, pp. 177-179, 2015

29. McCrea, I.; Aikio, A.; Alfonsi, L.; Belova, E.; Buchert, S.; Ciliverd, M.; Engler, N.; Gustavsson, B.; Heinselmann, C.; Kero, J.; Kosch, M.; **Lamy, H.**; Leyser, T.; Ogawa, Y.; Oksavik, K.; Pellinen-Wannberg, A.; Pitout, F.; Rapp, M.; Stanislawska, I.; Vierinen, J.
The science case for the EISCAT 3D radar
Progress in Earth and Planetary Science, 2, 21, 63, 2015, DOI: 10.1186/s40645-015-0051-8

30. Meftah, M.; Irbah, A.; Hauchecorne, A.; Corbard, T.; Turck-Chièze, S.; **Hochedez, J.-F.**; Boumier, P.; **Chevalier, A.**; **Dewitte, S.**; **Mekaoui, S.**; Salabert, D.
On the Determination and Constancy of the Solar Oblateness
Solar Physics, 290, pp. 673-687, 2015

31. Moon, K.; **Delouille, V.**; Hero III, A.O.
Meta learning of bounds on the Bayes classifier error
Proceeding of IEEE Signal Processing and SP Education workshop, 2015, DOI: 10.1109/DSP-SPE.2015.7369520

32. Morel, L.; **Pottiaux, E.**; Durand, F.; Fund, F.; Boniface, K.; de Olivera Junior, P.S.; Van Baelen, J.

Validity and behaviour of tropospheric gradients estimated by GPS in Corsica

Advances in Space Research, 55, 1, pp. 135-149, 2014, DOI: 10.1016/j.asr.2014.10.004

33. Morosan, D.E.; ...; **Magdalenic, J.**; and 51 co-authors
LOFAR tied-array imaging and spectroscopy of solar S bursts

Astronomy & Astrophysics, 580, A65, 2015, DOI: 10.1051/0004-6361/201526064

34. Möstl, C.; Rollett, T.; Frahm, R.A.; Liu, Y.D.; Long, D.M.; Colaninno, R.; Reiss, M.A.; Temmer, M.; Farrugia, C.J.; Posner, A.; Dumbovic, M.; Janvier, M.; Demoulin, P.; Boakes, P.; **Devos, A.**; **Kraaikamp, E.**; Mays, M.L.; Vrsnak, B.

Strong coronal channeling and interplanetary evolution of a solar storm up to the Earth and the Mars

Nature Communications, 6, 2015, DOI: 10.1038/ncomms8135

35. **Neefs, E.**; **Vandaele, A.C.**; **Drummond, R.**; **Thomas, I.**; **Berkenbosch, S.**; **Clairquin, R.**; **Delanoye, S.**; **Ristic, B.**; **Maes, J.**; **Bonnewijn, S.**; **Pieck, G.**; **Equeter, E.**; **Depiesse, C.**; **Daerden, F.**; and 35 co-authors

NOMAD spectrometers on the ExoMars trace gas orbiter mission: part 1 - design, manufacturing and testing of the infrared channels

Applied Optics 54, 28, pp. 8494-8520, 2015, DOI: <http://dx.doi.org/10.1364/AO.54.008494>

36. Pant, V.; **Dolla, L.**; Mazumder, R.; Banerjee, D.; Prasad, S.K.; Panditi, V.

Dynamics of on-disc plumes as observed with the Interface Region Imaging Spectrograph, the Atmospheric Imaging Assembly, and the Helioseismic and Magnetic Imager

The Astrophysical Journal, 807, pp. 71, 2015, DOI: 10.1088/0004-637X/807/1/71

37. **Parenti, S.**

Spectral Diagnostics of Cool Prominence and PCTR Optically Thin Plasmas

Solar Prominences, Astrophysics and Space Science Library, 415, pp. 61, 2015

38. Pasachoff, J.M.; Rusin, V.; Saniga, M.; Babcock, B.A.; Lu, M.; Davis, A.B.; Dantowitz, R.; Gaintatzis, P.; Seiradakis, J.H.; Voulgaris, A.; **Seaton, D.B.**; Shiota, K.

Structure and Dynamics of the 2012 November 13/14 Eclipse White-light Corona

The Astrophysical Journal, 800, 2015

39. **Ranvier S.**; **Lamy, H.**; **Anciaux, M.**; **Calders, S.**; **Gamby, E.**; **De Keyser, J.**

Instrumentation of the Belgian RAdio Meteor Stations (BRAMS)

Proceedings of ICEAA - IEEE APWC, Torino, Italy, September 2015

40. Reiss, M.A.; Hofmeister, S.J.; **De Visscher, R.**; Temmer, M.; Veronig, A. M.; **Delouille, V.**; **Mampaey, B.**; Ahammer, H.

Improvements on coronal hole detection in SDO/AIA images using supervised classification

Journal of Space Weather and Space Climate, 5, A23, 2015

41. Strugarek, A.; Janitzek, N.; Lee, A.; Löschl, P.; Seifert, B.; Hoilijoki, S.; **Kraaikamp, E.**; Isha Mrigakshi, A.; Philippe, T.; Spina, S.; Bröse, M.; Massahi, S.; OHalloran, L.; Pereira Blanco, V.; Stausland, C.; Escoubet, P.; Kargl, G.

A Space Weather mission concept: Observatories of the Solar Corona and Active Regions (OSCAR)

Journal of Space Weather and Space Climate, 5, A4, 2015

42. **Vandaele, A.C.**; **Willame, Y.**; **Depiesse, C.**; **Thomas, I.R.**; **Robert, S.**; **Bolsée, D.**; Patel, M.R.; Mason, J.P.; Leese, M.; Lesschaeve, S.; Antoine, P.; **Daerden, F.**; **Delanoye, S.**; **Drummond, R.**; **Neefs, E.**; **Ristic, B.**; Lopez-Moreno, J.-J.; Bellucci, G. and the NOMAD Team

Optical and radiometric models of the NOMAD instrument part I: the UVIS channel

Optics Express, 23, 23, pp. 30028-30042, 2015

43. **Vandaele, A.C.**; **Neefs, E.**; **Drummond, R.**; **Thomas, I.R.**; **Daerden, F.**; ...; **Bolsée, D.**; ...; **Delanoye, S.**; **Depiesse, C.**; ...; **Fussen, D.**; ...; **Mahieux, A.**; ...; **Neary, L.**; ...; **Ristic, B.**; **Robert, S.**; ...; **Wilquet, V.**; and 29 co-authors

Science objectives and performances of NOMAD, a spectrometer suite for the ExoMars TGO mission

Planetary and Space Science, 119, pp. 233-249, 2015, DOI: <http://dx.doi.org/10.1016/j.pss.2015.10.003>

44. Verbanac, G. ; **Pierrard, V.** ; Bandic, M. ; **Darrouzet, F.** ; Rauch, J.L. ; Décréau, P.

Relationship between plasmopause, solar wind and geomagnetic activity between 2007 and 2011 using Cluster data

Annales Geophysicae, 33, 1271-1283, 2015, DOI: 10.5194/angeo3312712015

45. **Verdini, A.**; Grappin, R.

Imprints of expansion on the local anisotropy of solar wind turbulence

The Astrophysical Journal Letters, 808, L34, 2015

46. **Verdini, A.**; Grappin, R.; Hellinger, P. ; Landi, S.; Müller, W.-C.

Anisotropy of third-order structure functions in MHD turbulence

The Astrophysical Journal, 804, pp. 119-232, 2015

47. **Verhulst, T.**; **Stankov, S.M.**

Ionospheric specification with analytical profilers:

Evidences of non-Chapman electron density distribution in the upper ionosphere

Advances in Space Research, 55, 8, pp. 2058-2069, 2015,
DOI: 10.1016/j.asr.2014.10.017

48. **Voitenko, Y.; Pierrard, V.**

Generation of Proton Beams by Non-uniform Solar Wind Turbulence

Solar Physics, 290, 1231, 2015, DOI: 10.1007/s11207-015-0661-8

49. **West, M.; Seaton, D.B.**

SWAP Observations of Post-flare Giant Arches in the Long-Duration 14 October 2014 Solar Eruption

The Astrophysical Journal Letters, 801, L6, 2015

50. Zhao, J.S.; **Voitenko, Y.**; **De Keyser, J.**; Wu, D.J.
Scalar and Vector Nonlinear Decays of Low-frequency Alfvén Waves

The Astrophysical Journal, 799, 222, 2015, DOI:
10.1088/0004-637X/799/2/222

51. Zhao, J.S.; **Voitenko, Y.**; Guo, Y.; Su, J.T.; Wu, D.J.
Nonlinear damping of Alfvén waves in the solar corona below 1.5 solar radii

The Astrophysical Journal, 811, 88, 2015, DOI:
10.1088/0004-637X/811/2/88

Presentations and posters at conferences

1. Aerts, W.; Baire, Q.; Bergeot, N.; Bruyninx, C.; Chevalier, J.-M.; Defraigne, P.; Legrand, J.; Pottiaux, E.; Roosbeek F.; Voet, P.
Belgian national report
EUREF Symposium, Leipzig, Germany, 3-5 June 2015
2. Altadill, D.; Paznukhov, V.; Blanch, E.; Galkin, I.; Verhulst, T.; Mielich, J.; Belehaki, A.; Reinisch, B.; Stankov, S.M.; Buresova, D.; Francis, M.
Results from D2D skymaps from Belgium to Spain: Challenges and chance to identify TIDs
ESWW12, Oostende, Belgium, 23-27 November 2015
3. Andries, J.
The SIDC and its Space weather services
STCE Workshop: Natural Hazard Assessment for Aviation, Brussels, Belgium, 2 June 2015
4. Andries, J.; Devos, A.; Berghmans, D.
RWC Belgium: learning from 15 years of operational Space Weather Services
ESWW12, Oostende, Belgium, 23-27 November 2015
5. Aragon-Angel, A.; Hernandez-Pajares, M.; Defraigne, P.; Bergeot, N.; Prieto-Cerdeira, R.
Modelling and Assessing Ionospheric Higher Order Terms for GNSS Signals
ION GNSS+, Tampa, USA, 14-18 September 2015
6. Barthélemy, M.; Lamy, H.; Lilensten, J.; Vialatte, A.
1er cru: A spectropolarimeter to measure the polarisation of auroral thermospheric emission spectra
EGU General Assembly 2015, Vienna, Austria, 13-17 April 2015 (poster)
7. Belehaki, A.; Reinisch, B.; Galkin, I.; Altadill, D.; Buresova, D.; Francis, M.; Mielich, J.; Paznukhov, V.; Stankov, S.M.
Pilot network for identification of travelling ionospheric disturbances
International Ionospheric Effects Symposium (IES), Alexandria, VA, USA, 12-14 May 2015
8. Belehaki, A.; Reinisch, B.; Galkin, I.; Altadill, D.; Buresova, D.; Francis, M.; Mielich, J.; Paznukhov, V.; Stankov, S.M.
Pilot network for identification of travelling ionospheric disturbances
1st URSI Atlantic Radio Science Conference (AT-RASC), Gran Canaria, Spain, 18-25 May 2015
9. BenMoussa, A.; Gissot, S.; Giordanengo, B.
Space-based instrument developments for UV solar observations, focus on detector technology
Solar Metrology, Needs and Methods II, Brussels, Belgium, 21-23 September 2015 (invited talk)
10. Bergeot, N.
GNSS et applications à la météorologie spatiale et à la recherche en Antarctique
Université Paris Diderot, Paris, France, 17 February 2015
11. Bergeot, N.; Chevalier, J.-M.; Bruyninx, C.
Climatological behavior of the ionospheric total electron content over Europe for the period 1998-2014
EGU General Assembly 2015, Vienna, Austria, 13-17 April 2015
12. Bergeot, N.; Chevalier, J.-M.; Bruyninx, C.
Performance of ROB's near real-time ionospheric product during normal and disturbed space weather periods
EGU General Assembly 2015, Vienna, Austria, 13-17 April 2015
13. Bergeot, N.; Chevalier, J.-M.; Bruyninx, C.
GNSS-based ionospheric monitoring
1st URSI Atlantic Radio Science Conference (AT-RASC), Gran Canaria, Spain, 18-25 May 2015
14. Bergeot, N.; Bruyninx, C.; Drews, R.; Pattyn, F.; Van Dam, T.; Tabibi, S.
GNSS in East Antarctica around the Princess Elisabeth Belgian base
SCAR Expert Group GRAPE (GNSS Research and Application for Polar Environment), Meeting at 1st URSI Atlantic Radio Science Conference (URSI AT-RASC), Gran Canaria, Spain, 18-25 May 2015
15. Bergeot, N.; Chevalier, J.-M.
Global Navigation Satellite System (GNSS) and Space Weather
STCE Workshop: Natural Hazard Assessment for Aviation, Brussels, Belgium, 2 June 2015
16. Berghmans, D.
SIDC tools
MADAWG splinter at the 6th Meeting of the Science Operation WG of Solar Orbiter, ESAC, Madrid, Spain, 19-22 January 2015
17. Bisi, M.; Davis, A.B.; Harrison, R.A.; Möstl, C.; Rouillard, A.P.; Bothmer, V.; Rodriguez, L.; Eastwood, J.P.; Kilpua, E.; Gallagher, P.T.; Odstrcil, D.
HELICATS: HELiospheric Cataloguing, Analysis and Techniques Service
3rd Remote Sensing of the Inner Heliosphere Space Weather Applications Workshop, Michoacan, Mexico, 20-24 October 2015 (poster)

18. Bolsée, D. et al.
The SOLAR/SOLSPEC project
Workshop “Six years of SOLAR/SOLSPEC mission on ISS. Achievements and prospects”, BIRA-IASB, Brussels, Belgium, 10-12 March 2015
19. Bolsée, D. et al.
IR solar measurements with SOLAR/SOLSPEC
Workshop “Six years of SOLAR/SOLSPEC mission on ISS. Achievements and prospects”, BIRA-IASB, Brussels, Belgium, 10-12 March 2015
20. Bolsée, D. et al.
The SOLAR/SOLSPEC project
PROMOPTICA annual event, BIRA-IASB, Brussels, Belgium, 31 March 2015
21. Bolsée, D. et al.
The SOLAR/SOLSPEC project
NOMAD SWT meeting, CSL, Liège, Belgium, 21 April 2015
22. Bolsée, D. et al.
The DPM (Data Processing Model) of SOLAR/SOLSPEC
SOLAR FST Meeting, ESTEC, The Netherlands, 4-5 June 2015
23. Bolsée, D. et al.
The Solar Spectral Irradiance in the Near IR
Solar Metrology, Needs and Methods II, Brussels, Belgium, 21-23 September 2015
24. Borremans, K.; Pierrard, V.
Dropout events
International Workshop on Energetic Particle Processes of the near Earth Space, Paris, France, 17-23 May 2015
25. Brenot, H.; Dick, G.; Dousa, J.; Kaplon, J.; Möller, G.; Morel, L.; Nahmani, S.; Pottiaux, E.; Santos, M.
WG1 ASYM: Asymmetry monitoring from GNSS
COST ES1206 - GNSS4SWEC: 2nd Workshop, Thessaloniki, Greece, 11-13 May 2015
26. Bruyninx, C.
EPN Densification: Meta-data Management and Web Pages
EUREF Symposium, Leipzig, Germany, 3-5 June 2015
27. Bruyninx, C.
EUREF Permanent GNSS Network
ENEON 1st workshop - Observing Europe: Networking the Earth Observation Networks in Europe, Paris, France, 21-22 September 2015 (invited talk)
28. Bruyninx, C.
News from the EPN Central Bureau
EUREF Analysis Centers Workshop, Bern, Switzerland, 14-15 October 2015
29. Cessateur, G.; Barthelemy, M.; De Keyser, J.; Dhooghe, F.; Loreau, J.; Maggiolo, R.; Gibbons, A.; Vaeck, N.; Altwegg, K.; Le Roy, L.; Berthelier, J.-J.; Calmonte, U.; Fuselier, S.; Hässig, M.; Rubin, M.; Gombosi, T.I.; Combi, M.
Space weather phenomena at Galilean moons and comets
European Planetary Science Congress 2015, La Cité des Congrès, Nantes, France, 27 September-02 October 2015 (invited talk)
30. Cessateur, G.; Loreau, J.; De Keyser, J.; Dhooghe, F.; Maggiolo, R.; Vaeck, N.; Urbain, X.; Palmeri, P.; Quinet, P.; Gibbons, A.; Gunell, H.
Updating reaction rates in the frame of planetary space weather
ESWW12, Oostende, Belgium, 23-27 November 2015 (poster)
31. Chevalier, J.-M.; Bergeot, N.; Marqué, C.; Aerts, W.; Bruyninx, C.
Effect of solar radio bursts on GNSS signal reception over Europe for the period 1999-2013
EGU General Assembly 2015, Vienna, Austria, 13-17 April 2015
32. Clette, F.; Lefèvre, L.
Re-calibrating the sunspot number: Diagnostics and implications
Sun-Climate Connections, Kiel, Germany, 16-19 March 2015
33. Clette, F.
Living in the sunshine : The source and role of light in the Sun-Earth relations
PROMOPTICA annual event, BIRA-IASB, Brussels, Belgium, 31 March 2015
34. Clette, F.; Lefèvre, L.; Svalgaard, L.; Cliver, E.W.; Vaquero, J.M.
The new Sunspot and Group Numbers: A full recalibration
IAU 29th General Assembly, Division E session, Honolulu, Hawaii, 3-14 August 2015 (invited talk)
35. Clette, F.; Lefèvre, L.
The new Sunspot Number: re-calibration, re-computation and implications for the solar cycle
IAU 29th General Assembly, Focus Meeting 13, Honolulu, Hawaii, 3-14 August 2015 (poster)
36. Clette, F.
400 years of Sunspot Numbers: A complete revision
Tubitak National Observatory, Akdeniz University, Antalya, Turkey, 16 September 2015 (invited talk)
37. Clette, F.; Lefèvre, L.
The revised sunspot number New properties and new data standards

Coimbra Solar Physics Meeting (CSPM), Coimbra, Portugal, 5-9 October 2015

38. Clette, F.

The new Sunspot Group numbers: Remaining issues and future work

Coimbra Solar Physics Meeting (CSPM), Coimbra, Portugal, 5-9 October 2015 (invited talk)

39. Clette, F.; Lefèvre, L.

New re-calibrated sunspot numbers and the past solar output

SORCE Sun-Climate Symposium, Savannah, GE, USA, 10-13 November 2015

40. Clette, F.; Lefèvre, L.

Implications and prospects for the new Sunspot Number
ESWW12 (working meeting), Oostende, Belgium, 23-27 November 2015

41. Clette, F.; Lefèvre, L.

Renewing our view to past solar activity: the new Sunspot Number series

ESWW12, Oostende, Belgium, 23-27 November 2015

42. Clette, F.

Cycle 24 in a 400-year perspective: The Sunspot Number record

ESWW12 (working meeting), Oostende, Belgium, 23-27 November 2015 (invited talk)

43. Dammasch, I.E.; Dominique, M.

Long-term variability of LYRA data

Solar Metrology, Needs and Methods II, Brussels, Belgium, 21-23 September 2015

44. Dammasch, I.E.; Dominique, M.

LYRA flare probabilities service and its performance measure

ESWW12, Oostende, Belgium, 23-27 November 2015 (poster)

45. Dammasch, I.E.; Dominique, M.

LYRA experiences for future space weather instruments

ESWW12, Oostende, Belgium, 23-27 November 2015 (poster)

46. De Cruz, L.; Duerinckx, A.; Pottiaux, E.

GNSS Assimilation In NWP: Case Studies For Belgium

COST ES1206 - GNSS4SWEC: 2nd Workshop, Thessaloniki, Greece, 11-13 May 2015

47. Defraigne, P.; Huang, W.; Bergeot, N.; Chevalier, J.M.;

Cerretto, G.; Cantoni, E.; Perucca, A.; Mudrak, A.

Galileo Signals for Time and Frequency Users

5th International Colloquium Scientific and Fundamental Aspects of the Galileo Programme, Braunschweig, Germany, 27-29 October 2015

48. De Groof, A.; Seaton, D.B.; Rachmeler, L.A.; Berghmans, D.

PROBA2/SWAP EUV images of the large-scale EUV corona up to 3 solar radii: Can we close the gap in coronal magnetic field structure between 1.3 and 2.5 solar radii?

Joint American Astronomical Society/American Geophysical Union Triennial Earth-Sun Summit, meeting #1, #409.01, Indianapolis, IN, USA, 26-30 April 2015

49. De Keyser, J.; Maes, L.; Maggiolo, R.; Haaland, S.
Exploration of tangential discontinuity structure of the dawn and dusk flank magnetopause

EGU General Assembly 2015, Vienna, Austria, 13-17 April 2015 (poster)

50. De Keyser, J.; Maes, L.; Haaland, S.; Maggiolo, R.
Understanding dawn-dusk asymmetry at the magnetopause

ESWW12, Oostende, Belgium, 23-27 November 2015 (poster)

51. Delouille, V.; Mampaey, B.; Haberreiter, M.

Error analysis on determination of filling factors for EUV irradiance reconstruction

SOLID 3rd consortium meeting, Thessaloniki, Greece, 5-8 October 2015

52. Demoulin, P.; Fussen, D.; Pieroux, D.; Ranvier, S.; Ancliaux, M.; Cardoen, P.; Bonnewijn, S.; Vanhellemont, F.; Dekemper, E.; De Keyser, J.

PICASSO, a scientific CubeSat mission for Earth observation

7th European Cubesat Symposium, Liège, Belgium, 9-11 September 2015

53. De Troch, R.; Van Schaeybroeck, B.; Termonia, P.; Willems, P.; Van Lipzig, N.; Van Ypersele, J.-P.; Fettweis, X.; De Ridder, K.; Gobin, A.; Stavrakou, T.; Luyten, P.; Pottiaux, E.

Combining the regional downscaling expertise in Belgium: CORDEX and beyond

6th Belgian Geography days, Brussels, Belgium, 13-14 November 2015 (poster)

54. Devos, A.; Andries, J.

The future role of the SWE Coordination Centre: review and recommendations

ESWW12, Oostende, Belgium, 23-27 November 2015

55. Devos, A.; Verbeeck, C.; Andries, J.

Verification of forecast probabilities at RWC Belgium

ESWW12, Oostende, Belgium, 23-27 November 2015

56. Dewitte, S.

The Value of the Solar Constant

SORCE Sun-Climate Symposium, Savannah, GE, USA, 10-13 November 2015

57. D'Huys, E.; Seaton, D.B.; SWAP Team
SWAP Status Update
ESWW12 (PROBA2 Science Working Team), Oostende, Belgium, 23-27 November 2015
58. Dias, B.; Magin, T.; Chatelain, P.; De Keyser, J.; Lamy, H.
Simulation of the atmospheric entry of meteors with application to radio detection
VKI PhD Student Symposium, von Karman Institute for Fluid Dynamics, St.-Genesius-Rode, Belgium, 11-13 March 2015 (poster)
59. Dias, B.; Turchi, A.; Magin, T.; De Keyser, J.; Lamy, H.
Towards a physics-based model for meteor interaction with Earth's atmosphere
ESWW12, Oostende, Belgium, 23-27 November 2015 (poster)
60. Dolla, L.
PROBA-3/ASPIICS operations concept
PROBA-3 SWT-2 meeting, Brussels, Belgium, 25-26 March 2015
61. Dolla, L.
PROBA-3/ASPIICS Green line filter: spectral purity, wavelength center...
PROBA-3 SWT-3 meeting, ESTEC, the Netherlands, 4-5 November 2015
62. Dolla, L.; Zhukov, A.N.; Rodriguez, L.; Mierla, M.; Janssens, J.; Bourgoignie, B.; ASPIICS Consortium
PROBA-3/ASPIICS Science Activity Plan
PROBA-3 SWT-3 meeting, ESTEC, the Netherlands, 4-5 November 2015
63. Dominique, M.
Sub-minute quasi-periodic pulsations in solar flares
CHARM meeting, Brussels, Belgium, 4-5 June 2015
64. Dominique, M.; Dammasch, I.E.; Ryan, D.F.; Wauters, L.; Katsiyannis, A.C.
LYRA status update
PROBA2 SWT, Brussels, Belgium, 30 June 2015
65. Dominique, M.; Dammasch, I.E.; Wauters, L.; BenMoussa, A.; Jones, A.R.
Progress towards understanding the degradation affecting the PROBA2/LYRA instrument
Solar Metrology, Needs and Methods II, Brussels, Belgium, 21-23 September 2015
66. Dominique, M.; Seaton, D.B.; Berghmans, D.; Katsiyannis, A.C.; West, M.; Dolla, L.; Ryan, D. F.; Bonte, K.; Kretzschmar, M.; Dammasch, I.E.; Wauters, L.; Rachmeler, L.A.
PROBA2: A Micro-Satellite Observing the Sun
AGU Fall Meeting, San Francisco, USA, 14-18 December 2015 (poster)
67. Eastwood, J.P.; Krupar, V.; Bisi, M.; Magdalenic, J.; Forsyth, R.; Good, S.W.
Assessing the complementary nature of radio measurements of solar wind transients: HELCATS WP7
HELCATS First Annual Open Workshop, Gottingen, Germany, 19-22 May 2015 (poster)
68. Gissot, S.; Giordanengo, B.; BenMoussa, A.
EUV characterization of (P43/P46) phosphor coated front-side illuminated CMOS image sensors for solar observations
290th PTB-Seminar VUV and EUV Metrology, Berlin, Germany, 5-6 November 2015
69. Gunell, H.; Andersson, L.; De Keyser, J.; Mann, I.
Repeatedly reforming double layers in the return current region of the aurora: model calculations and laboratory simulations
International Workshop 2015 on the Interrelationship between Plasma Experiments in the Laboratory and in Space (IPELS2015), Pitlochry, Scotland, UK, 23-28 August 2015 (invited talk)
70. Gunell, H.; Slapak, R.; Hamrin, M.; Nilsson, H.
Inverse ion cyclotron damping in Earth's cusp
International Workshop 2015 on the Interrelationship between Plasma Experiments in the Laboratory and in Space (IPELS2015), Pitlochry, Scotland, UK, 23-28 August 2015 (poster)
71. Haberreiter, M.; Delouille, V.; Del Zanna, G.; Dammasch, I.E.; Dominique, M.; Dudok de Wit, T.; Ermolli, I.; Jones, A.R.; Kretzschmar, M.; Mampaey, B.; Schaefer, R.; Schmidtke, G.; Schöll, M.; Thuillier, G.; Verbeeck, C.; Wieman, S.; Woods, T.; Schmutz, W.
Modeling the EUV/UV irradiance within the FP7 SOLID Project
EGU General Assembly 2015, Vienna, Austria, 13-17 April 2015 (poster)
72. Harrison, R.A.; Davis, A.B.; Möstl, C.; Rouillard, A.P.; Bothmer, V.; Rodriguez, L.; Kilpua, E.; Gallagher, P.T.; Odstrcil, D.
HELCATS – Heliospheric Cataloguing, Analysis and Technique Service
ESWW12, Oostende, Belgium, 23-27 November 2015
73. Inglis, A.; Ireland, J.; Dominique, M.
How can we interpret and understand pulsations in solar flare emission? A Bayesian model comparison approach
Joint American Astronomical Society/American Geophysical Union Triennial Earth-Sun Summit, meeting #1, #409.01, Indianapolis, IN, USA, 26-30 April 2015

74. Jones, J.; Guerova, G.; Dousa, J.; Dick, G.; de Haan, S.; Pottiaux, E.; Bock, O.; Pacione, R.
COST Action ES1206: GNSS for Severe Weather and Climate (GNSS4SWEC)
EGU General Assembly 2015, Vienna, Austria, 13-17 April 2015 (poster)
75. Jones, J.; Guerova, G.; Dousa, J.; Dick, G.; De Haan, S.; Pottiaux, E.; Bock, O.; Pacione, R.
COST Action ES1206: Advanced Global Navigation Satellite Systems tropospheric products for monitoring severe weather events and climate (GNSS4SWEC)
International Union of Geodesy and Geophysics (IUGG), General Assembly 2015, Prague, Czech Republic, 22 June-2 July 2015
76. Jones, J.; Guerova, G.; Dousa, J.; Dick, G.; De Haan, S.; Pottiaux, E.; Bock, O.; Pacione, R.
Satellite Systems Tropospheric Products for Monitoring Severe Weather Events and Climate (GNSS4SWEC)
5th International Colloquium Scientific and Fundamental Aspects of the Galileo Programme, Braunschweig, Germany, 27-29 October 2015
77. Katsiyannis, A.C.; Dominique, M.; De Keyser, J.; Kruglanski, M.; De Donder, E.; BenMoussa, A.; Berghmans, D.
LYRA detections of Aurora events
ESWW12, Oostende, Belgium, 23-27 November 2015 (poster)
78. Katsiyannis, A.C.; De Keyser, J.; Kruglanski, M.; De Donder, E.; BenMoussa, A.; Berghmans, D.
Space weather effects on LYRA
ESWW12, Oostende, Belgium, 23-27 November 2015 (poster)
79. Katsiyannis, A.C.; Dominique, M.; De Keyser, J.; Berghmans, D.; Kruglanski, M.; Dammasch, I.E.; Borremans, K.; De Donder, E.; BenMoussa, A.
Detection of EUV/Soft X-ray bremsstrahlung emission at terrestrial altitudes above 750 km
AGU Fall Meeting, San Francisco, USA, 14-18 December 2015 (poster)
80. Kenyeres, A.; Horvath, T.; Bruyninx, C.; Mesmaker, D.; Caporali, A.; Baron, A.; De Doncker, F.; Droscak, B.; Duret, A.; Franke, P.; Georgiev, I.; Gianniu, M.; Hansen, D.; Huisman, L.; Jumare, I.; Nagl, J.L.; Phihlak, P.; Stangl, G.; Valdes, M.; Szafranek, K.; Figurski, M.; Ryczywolsk, M.
Recent Advances in the EPN densification: An overview
EUREF Symposium, Leipzig, Germany, 3-5 June 2015
81. Kenyeres, A.; Altamimi, Z.; Bruyninx, C.; Caporali, A.; Lidberg M.; Stangl, G.
EPN Densification: Status and Actions
EUREF Analysis Centers Workshop, Bern, Switzerland, 14-15 October 2015
82. Kilpua, E.; Isavnin, A.; Vourlidis, A.; Koskinen, H.E.J.; Rodriguez, L.
Internal structure of interplanetary coronal mass ejections and relation to remote sensing observations
HELCASTS First Annual Open Workshop, Gottingen, Germany, 19-22 May 2015
83. Kotov, D.; Richards, P.; Truhlik, V.; Stankov, S.M.; Bogomaz, O.; Chernogor, L.; Domnin, I.
Plasmasphere refilling rates as deduced from Ukraine incoherent scatter radar data by FLIP simulation for the last solar minimum
AGU-CGU Joint Assembly, Montreal, Canada, 3-7 May 2015
84. Kraaikamp, E.; Verbeeck, C.
Solar Demon: Detecting Flares, Dimmings, and EUV waves in near real-time on SDO-AIA images
ESWW12, Oostende, Belgium, 23-27 November 2015 (poster)
85. Kraaikamp, E.; Verbeeck, C.
Solar Demon: Detecting Flares, Dimmings, and EUV waves in near real-time on SDO-AIA images
ESWW12, Oostende, Belgium, 23-27 November 2015
86. Kruglanski, M.; De Donder, E.; Glover, A.; Borries, C.; Janssens, J.
Services for GNSS users within the ESA Space Situational Awareness Space Weather Service Network
IAIN World Congress 2015, Prague, Czech Republic, 20-23 October 2015
87. Krupar, V.; Bothmer, V.; Davies, J.; Eastwood, J.P.; Forsyth, R.; Kruparova, O.; Magdalenic, J.; Maksimovic, M.; Santolik, O.; Soucek, J.; Vourlidis, A.
Radio Triangulation of Type II Bursts Associated with a CME - CME Interaction
AGU Fall Meeting, San Francisco, USA, 14-18 December 2015 (poster)
88. Laffineur, Q.; Haeffelin, M.
New development in fog prediction capabilities of ALC at two different sites
COST ES1303-TOPROF 4th MC and WG meeting, Granada, Spain, 5-7 May 2015
89. Laffineur, Q.; De Backer, H.; Delclocq, A.
Benefit of a LIDAR-ceilometer network for aviation
STCE Workshop: Natural Hazard Assessment for Aviation, Brussels, Belgium, 2 June 2015
90. Laffineur, Q.; Haeffelin, M.; Dupont, J.-C.; Bravo-Aranda, J.A.; Casquero-Vera, J.A.
Task 6: Update and overview of fog activities
COST ES1303-TOPROF 5th MC and WG meeting, Toulouse, France, 19-21 October 2015

91. Lamy, H.
BRAMS: a radio network using forward scatter to monitor meteoroid activity
ESWW12, Oostende, Belgium, 23-27 November 2015
(invited talk)
92. Lamy, H.; Barthélemy, M.
A New Spectropolarimeter to Study the Polarization of Earth's Auroral Emission Lines
AGU Fall Meeting, San Francisco, USA, 14-18 December 2015 (poster)
93. Lefèvre, L.; Clette, F.
Going beyond the international Sunspot Number
Sun-Climate Connections, Kiel, Germany, 16-19 March 2015 (poster)
94. Lefèvre, L.; Carrasco, Victor; Vaquero, J.M.; Gallego, Maricruz
Equivalence relations between the Cortie and Zurich sunspot group morphological classifications
Sun-Climate Connections, Kiel, Germany, 16-19 March 2015 (poster)
95. Lefèvre, L.; Clette, F.
The new and improved Sunspot Number
Solar Metrology, Needs and Methods II, Brussels, Belgium, 21-23 September 2015 (invited talk)
96. Lefèvre, L.
Sunspot Information and error bars
SOLID 3rd consortium meeting, Thessaloniki, Greece, 5-8 October 2015
97. Lefèvre, L.; Cliver, E.W.
The new and improved Sunspot Number
6th BBC SWS Regional Network conference, Athens, Greece, 2-6 November 2015 (invited talk)
98. Lopez Rosson, G.; Pierrard, V.; Borremans, K.; Lemaire, J.
EPT data analysis : Radiation belts flux variations related with SEP events and geomagnetic storms
IMC3 (Inner Magnetosphere Coupling), Los Angeles, USA, 23-27 March 2015
99. Lopez Rosson, G.; Borremans, K.; Dierckxsens, M.; Pierrard, V.; Benck, S.; Cyamukungu, M.; Borisov, S.; Nieminen, P.; Grégoire, G.; Lemaire, J.
Entry of ultrarelativistic solar energetic electrons into the Van Allen radiation belts: Observations and theory
26th IUGG General Assembly, Prague, Czech Republic, 22 June-02 July 2015
100. Magdalenic, J.; Marqué, C.; Krupar, V.; Mierla, M.; Zhukov, A.N.; Rodriguez, L.; Maksimovic, M.; Cecconi, B.
Tracking the CME-driven shock wave on 2012 March 5 and radio triangulation of associated radio emission
HELCASTS First Annual Open Workshop, Gottingen, Germany, 19-22 May 2015
101. Magdalenic, J.; Marqué, C.
Fine structures of the type II radio burst as seen by LOFAR
9th Annual Meeting of the KSP "Solar Physics and Space Weather with LOFAR", Brussels, Belgium, 26-27 May, 2015
102. Magdalenic, J.; SIDC forecasters
Space weather: The state of the art and where to go
AOGS (Asia Oceanic Geosciences Society) 12th Annual meeting, Singapore, 2-7 August 2015 (invited talk)
103. Magdalenic, J.; Temmer, M.; Krupar, V.; Marqué, C.; Vrsnak, B.; Veronig, A. M.
Radio triangulation of the radio signatures of a CME-CME interaction
AOGS (Asia Oceanic Geosciences Society) 12th Annual meeting, Singapore, 2-7 August 2015 (poster)
104. Magdalenic, J.; Martinez Picar, A.; Marqué, C.
Solar Radio Observations by the Royal Observatory of Belgium - HUMAIN Radioastronomy Station
ESWW12, Oostende, Belgium, 23-27 November 2015 (poster)
105. Magdalenic, J.; Janssens, J.; SIDC forecasters team
Solar activity on November 4, 2015 and the associated space weather
ESWW12, Oostende, Belgium, 23-27 November 2015
106. Magdalenic, J.; Temmer, M.; Krupar, V.; Marqué, C.; Veronig, A.M.; Vrsnak, B.
Radio-triangulation of an unusual solar radio burst possibly originating from the CME-CME interaction
ESWW12, Oostende, Belgium, 23-27 November 2015
107. Malisse, V. ; Verbeeck, C.
STAFF: Solar Timelines Viewer for AFFECTS
ESWW12, Oostende, Belgium, 23-27 November 2015 (poster)
108. Marqué, C.
Solar radio data: spectra, images, observations
CESRA Radio Summer School 2015, Glasgow, UK, 24-28 August 2015 (invited talk)
109. Maruyama, N.; Richards, P.G.; Fedrizzi, M.; Fuller-Rowell, T.J.; Fang, T.-W.; Codrescu, M.; Pierrard, V.; Denton, M.
Ionosphere-Plasmasphere coupling using the ionosphere-plasmasphere electrodynamics (IPE) model
AGU Fall Meeting, San Francisco, USA, 14-18 December 2015 (poster)

110. Mazzino, M.L.; Cully, C.M.; Benck, S; Cyamukungu, M.; Borisov, S; Pierrard, V.
Investigation of Energetic Particle Precipitation using the Array for Broadband Observations of VLF/ELF Emissions (ABOVE) and the Energetic Particle Telescope (EPT), Ionosphere-Plasmasphere coupling using the ionosphere-plasmasphere-electrodynamics (IPE) model
AGU Fall Meeting, San Francisco, USA, 14-18 December 2015
111. Mero, B.; Quillien, K.A.; McRobb, M.; Chesi, S.; Marshall, R.; Gow, A.; Clark, C.; Anciaux, M.; Cardoen, P.; De Keyser, J.; Demoulin, P.; Fussen, D.; Pieroux, D.; Ranvier, S.
PICASSO: A State of the Art CubeSat
29th Annual AIAA/USU Conference on Small Satellites, Logan, Utah, USA, 8-13 August 2015
112. Mierla, M.
Highlights of STEREO
Der Deutschen Physikalischen Gesellschaft meeting, Wuppertal, Germany, 9-13 March 2015 (invited talk)
113. Mierla, M.; Kilpua, E.; Rodriguez, L.; Zhukov, A.N.
Analysis of CMEs-ICMEs on the ascending phase of SC24
ESWW12, Oostende, Belgium, 23-27 November 2015
114. Morel, L.; Pottiaux, E.; Durand, F.; Fund, F.; Durand, S.; Boniface, K.; Follin, J.-M.; de Oliveira Junior, P. S.; Van Baelen, J.
Global validity and behaviour of tropospheric gradients estimated by GPS
COST ES1206 - GNSS4SWEC: 2nd Workshop, Thessaloniki, Greece, 11-13 May 2015
115. Morel, L.; Pottiaux, E.; Durand, F.; Fund, F.; Follin, J.-M.; Durand, S.; Boniface, K.; de Oliveira Junior, P.S.; Van Baelen, J.
Global validity and behaviour of tropospheric gradients estimated by GPS
International Union of Geodesy and Geophysics (IUGG), General Assembly 2015, Prague, Czech Republic, 22 June-2 July 2015 (poster)
116. Moschou, S.; Pierrard, V.; Pomoel, J.; Keppens, R.
Solar wind modelling: MHD and kinetic treatments with kappa distributions for the electrons
AGU Fall Meeting, San Francisco, USA, 14-18 December 2015 (poster)
117. Möstl, C.; Rollett, T.; Frahm, R.A.; Liu, Ying D.; Long, D.M.; Colaninno, R.; Reiss, M.A.; Temmer, M.; Farrugia, C.J.; Posner, A.; Dumbovic, M.; Janvier, M.; Demoulin, P.; Boakes, P.; Devos, A.; Kraaikamp, E.; Mays, M.L.; Vrsnak, B.
Strong coronal deflection of a CME and its interplanetary evolution to Earth and Mars
EGU General Assembly 2015, Vienna, Austria, 13-17 April 2015 (poster)
118. Nevens, S.
TSI Reconstruction over the Last 300 Years
SORCE Sun-Climate Symposium, Savannah, GE, USA, 10-13 November 2015
119. Nicula, B.; Verstringe, F.; Bourgoignie, B.; Berghmans, D.; Marqué, C.; Jiggins, P.; Mueller, D.
Space Weather Helioviewer
ESWW12, Oostende, Belgium, 23-27 November 2015
120. Pacione, R.; Jones, J.; Van Malderen, R.; Bock, O.
Collaborations in GNSS sphere with other projects (GNSS4SWC, E-GVAP)
7th GRUAN Implementation-Coordination Meeting, Matera, Italy, 23-27 February 2015
121. Pacione, R. ; Jones, J. ; Guerova, G. ; Dousa, J. ; Dick, G. ; De Haan, S. ; Pottiaux, E. ; Bock, O. ; Elgered, G. ; Vedel, H.
COST Action ES1206 "Advanced Global Navigation Satellite Systems tropospheric products for monitoring severe weather events and climate (GNSS4SWEC)"
EUREF Symposium, Leipzig, Germany, 3-5 June 2015
122. Pierrard, V.; Moschou, S.
Influence of suprathermal electrons on the acceleration of solar wind particles
International Astrophysics Conference, Tampa Bay, USA, 20-24 April 2015 (invited talk)
123. Pierrard, V.; Verbanac, G.; Bandic, M.; Darrouzet, F.
Relationship between plasmopause obtained from Cluster, solar wind and geomagnetic activity
AGU-CGU Joint Assembly, Montreal, Canada, 3-7 May 2015 (poster)
124. Pierrard, V. ; Darrouzet, F. ; Borremans, K. ; Lopez Rosson, G.
Space weather effects in the inner magnetosphere: Plasmasphere and radiation belts dynamics during geomagnetic storms
1st URSI Atlantic Radio Science Conference (AT-RASC), Gran Canaria, Spain, 18-25 May 2015
125. Pierrard, V.
Study of the evolution of the velocity distribution functions of the solar wind particles as a function of the radial distance
Solar Orbiter and Solar Probe+, Florence, Italy, 24 September 2015
126. Pierrard, V.; Darrouzet, F.; Lopez Rosson, G.
Space weather observations to study the dynamics of the plasmopause and of the inner magnetosphere
ESWW12, Oostende, Belgium, 23-27 November 2015 (poster)

127. Pierrard, V.; Moschou, S.; Lemaire, J.
Plasmaspheric depletion and refilling after geomagnetic storms in the dynamic model of the plasmasphere
AGU Fall Meeting, San Francisco, USA, 14-18 December 2015 (invited talk)
128. Poedts, S.; Pomoell, J.; Verstringe, F.; Andries, J.; Berghmans, D.
Euhforia, European Heliospheric Forecasting Information Asset
7th meeting of the Science Operations WG of Solar Orbiter, ESAC, Madrid, 2015
129. Pottiaux, E.
GNSS Reprocessing For CORDEX.Be High-Resolution Climate Model Runs Verification
CORDEX.be: Kick-off Meeting, Brussels, Belgium, 31 March 2015
130. Pottiaux, E.; Dousa, J.; Vaclavovic, P.; Bruyninx, C.
Estimating troposphere parameters using real-time PPP: First results from ROB's demonstration campaign
COST ES1206 - GNSS4SWEC: 2nd Workshop, Thessaloniki, Greece, 11-13 May 2015
131. Pottiaux, E.; Termonia, P.; Willems, P.; Van Lipzig, N.; Van Ypersele, J.-P.; Fettweis, X.; De Ridder, K.; Gobin, A.; Stavrakou, T.; Luyten, P.; Van Schaeybroeck, B.; Bruyninx, C.
GNSS Re-processing For The Verification of Belgian High-Resolution Climate Model Runs
COST ES1206 - GNSS4SWEC: 2nd Workshop, Thessaloniki, Greece, 11-13 May 2015
132. Pottiaux, E.; Dousa, J.; Vaclavovic, P.; Bruyninx, C.
First Results of the Real-Time Multi-GNSS Troposphere Parameters Demonstration Campaign at the Royal Observatory of Belgium
International Union of Geodesy and Geophysics (IUGG), General Assembly 2015, Prague, Czech Republic, 22 June-2 July 2015
133. Pottiaux, E.; De Haan, S.
COST ES1206 (GNSS4SWEC) Working Group Meeting Wroclaw, Poland. WG2 Session: Report and Coordination
COST ES1206 - GNSS4SWEC : 4th Working Group Meeting, Wroclaw, Poland, 29 September-1 October 2015
134. Pottiaux, E.; Van Malderen, R.
Homogenization of GNSS time series. COST Action GNSS4SWEC sub-WG3 activity.
COST ES1206 - GNSS4SWEC : 4th Working Group Meeting, Wroclaw, Poland, 29 September-1 October 2015
135. Pottiaux, E.; Van Malderen, R.; Brenot, H.
COST ES1206 (GNSS4SWEC) M.C. Meeting Wroclaw, Poland: National Report of Belgium
136. Pottiaux, E.
GNSS Activities at ROB in Support of Meteorology and Climate: Current Status and Plans for E-GVAP and COST ES1206 (GNSS4SWEC)
3rd E-GVAP III Joint Expert Team Meeting, Wroclaw, Poland, 1-2 October 2015
137. Pottiaux, E.; Bruyninx, C.; Legrand, J.; Baire, Q.; Chevalier, J.-M.; Bergeot, N.
GNSS R&D and Services at ROB: Infrastructure, Challenges and Needs
E-Infrastructures in Belgium, Brussels, Belgium, 14 December 2015
138. Rachmeler, L.A.
Image Acquisition (ASPIICS)
PROBA-3 SWT-2 meeting, Brussels, Belgium, 25-26 March 2015
139. Rachmeler, L.A.; Guennou, C.; Seaton, D.B.; Auchere, F.
Southern Polar field reversal as revealed by a Pseudostreamer
SHINE (Solar Heliospheric INTERplanetary Environment), Stowe, VT, USA, 6-10 July 2015 (poster)
140. Rachmeler, L.A.
Coronal Observations
ISSI workshop on global, non-potential magnetic models of the solar corona, Bern, Switzerland, 24-28 August 2015
141. Ranvier, S.; Cardoen, P.; De Keyser, J.
Development of the Scientific Instruments for the PICASSO Mission
EGU General Assembly 2015, Vienna, Austria, 13-17 April 2015 (poster)
142. Ranvier, S.; De Keyser, J.; Cardoen, P.
Testing of the Sweeping Langmuir Probe (SLP) Instrument for the PICASSO Mission
International Workshop 2015 on the Interrelationship between Plasma Experiments in the Laboratory and in Space (IPELS2015), Pitlochry, Scotland, UK, 23-28 August 2015 (poster)
143. Ranvier, S.; De Keyser, J.; Cardoen, P.; Anciaux, M.; Gamby, E.; Pieroux, D.; Fussen, D.; Echim, M.; Lamy, H.; Gunell, H.
Space weather science with SLP on board PICASSO
ESWW12, Oostende, Belgium, 23-27 November 2015
144. Rodriguez, L.
WP2 Update: automatic CME identification
HELCASTS First Annual Open Workshop, Gottingen, Germany, 19-22 May 2015

145. Rodriguez, L.
WP2 Update: automatic CME identification
HELCASTS 3rd Bi-annual Steering Committee Meeting,
Helsinki, 3-4 November 2015
146. Rodriguez, L.; Willems, S.; Pant, V.; Mierla, M.; Devos, A.
Automatic detection of CMEs in STEREO-HI data
ESWW12, Oostende, Belgium, 23-27 November 2015
147. Ryan, D.F.; Machol, J.; Dominique, M.; Dammasch, I.E.
Lyman- α data from LYRA and GOES for use in flare studies
PROBA2 SWT, Brussels, Belgium, 30 June 2015
148. Sapundjiev, D.; Stankov, S.M.; Jodogne, J.C.
On the optimisation of the construction of a ground-based neutron monitor for galactic cosmic ray monitoring and space weather applications
International Cosmic Ray Conference (ICRC), The Hague, The Netherlands, 30 July-6 August 2015
149. Sapundjiev, D.; Stankov, S.M.
Ionospheric critical frequency prediction service based on digisonde measurements at Dourbes
ESWW12, Oostende, Belgium, 23-27 November 2015
150. Sapundjiev, D.; Steigies, C.; Verhulst, T.; Jodogne, J.C.; Stankov, S.M.
Upgrading the Dourbes cosmic ray observatory for research and development of improved space weather monitoring services
ESWW12, Oostende, Belgium, 23-27 November 2015
151. Seaton, D.B.; Berghmans, D.; De Groof, A.; Halain, J.P.; Nicula, B.; Rachmeler, L.A.
Lessons Learned in Five Years of Observations with the EUV Solar Telescope SWAP onboard PROBA2
Measurement Techniques in Solar and Space Physics, NCAR, Boulder, Colorado, USA, 20-24 April 2015
152. Seaton, D.B.; West, M.
PROBA2/SWAP Observations of the Unusual Activity of AR12192
Joint American Astronomical Society/American Geophysical Union Triennial Earth-Sun Summit, meeting #1, #409.01, Indianapolis, IN, USA, 26-30 April 2015
- SSCC Consortium (P2SWE-VI)
SSA Space Weather Coordination Centre
ESWW12, Oostende, Belgium, 23-27 November 2015
153. Thompson, B.; DeRosa, M.L.; Fisher, R.R.; Krista, L.D.; Young Kwon, R.; Mason, J.P.; Mays, M.L.; Nitta, N.V.; Webb, D.F.; West, M.
What Do EUV Dimmings Tell Us About CME Topology
Joint American Astronomical Society/American Geophysical Union Triennial Earth-Sun Summit, meeting #1, #212.01, Indianapolis, IN, USA, 26-30 April 2015
154. Van Malderen, R.; Pottiaux, E.; Brenot, H.; Beirle, S.; Wagner, T.; De Backer, H.; Bruyninx, C.
Assessment of IGS repro1 IWV trends by comparison with ERA-interim and GOMESCIA satellite data
COST ES1206 - GNSS4SWEC: 2nd Workshop, Thessaloniki, Greece, 11-13 May 2015
155. Verbeeck, C.
Lessons learned from SOWG-6 SOC planning exercise
15th EUI Consortium Meeting, MSSL, Guildford, UK, 3-5 March 2015
156. Verbeeck, C.
Live space weather forecast
ESWW12, Oostende, Belgium, 23-27 November 2015
157. Verhulst, T.; Stankov, S.M.
Ionosonde measurements of dynamic characteristics and inhomogeneities of the ionosphere
1st URSI Atlantic Radio Science Conference (AT-RASC), Gran Canaria, Spain, 18-25 May 2015
158. Voitenko, Y.; De Keyser, J.; Pierrard, V.; Zhao, J.; Malovichko, P.; Wu, D.
Alfvénic turbulence and ion beams
STORM-SHOCK meeting, Brussels, Belgium, 24-25 March 2015
159. Voitenko, Y.; Melnik, V.N.; Pierrard, V.
Bursts of kinetic Alfvén waves and coronal radio emission at 2-3 solar radii
1st URSI Atlantic Radio Science Conference (AT-RASC), Gran Canaria, Spain, 18-25 May 2015
160. Voitenko, Y.; Pierrard, V.; De Keyser, J.
Alfvénic Turbulence and Proton Beams in the Solar Wind
AOGS (Asia Oceanic Geosciences Society) 12th Annual meeting, Singapore, 2-7 August 2015 (invited talk)
161. Voitenko, Y.; Melnik, V.; Pierrard, V.; Brazhenko, A.; Frantsuzenko, A.
Probing Solar Plasmas and Waves by Coronal Radio Emission at 2-3 Solar Radii
AOGS (Asia Oceanic Geosciences Society) 12th Annual meeting, Singapore, 2-7 August 2015
162. Voitenko, Y.
Alfvénic Turbulence and Related Phenomena in Space Plasmas
UKUS-2015 Third UK-Ukraine-Spain Meeting on Solar Physics and Space Science, Lviv, Ukraine, 7-11 September 2015 (invited talk)
163. Voitenko, Y.; De Keyser, J.; Zhao, J.; Pierrard, V.

Turbulence Generated by Tail Collisions of Kinetic Alfvén Waves

THESOW-2015 Conference on Turbulence and Heating in the Solar Wind, Cargese, Corsica, France, 21-25 September 2015

164. Voitenko, Y.; Melnik, V.; Pierrard, V.; Brazhenko, A.; Frantsuzenko, A.

Narrow-band Bursts of Decameter Radio Emission From the Solar Corona

ESWW12, Oostende, Belgium, 23-27 November 2015

165. Wauters, L.; Dominique, M.; Dammasch, I.E.

Mid-term periodicities of LYRA data spectrum

Solar Metrology, Needs and Methods II, Brussels, Belgium, 21-23 September 2015

166. West, M.

PROBA2 a Space Weather Tool

Science from an Operational Mission: An L5 Consortium Meeting, London, UK, 11-14 May 2015

167. West, M.; Seaton, D.B.

SWAP IRIS Observations of Post-Flare Giant Arches

IRIS-4 workshop, Boulder, CO, USA, 18-22 May 2015 (poster)

168. West, M.; Seaton, D.B.

SWAP Observations of Post-flare Loops and the Effects of Background Coronal Conditions

Coronal Loop Workshop VII, Cambridge, UK, 21-23 July 2015 (poster)

169. West, M.; Seaton, D.B.

SWAP Observations of Post-Flare Giant Arches and the Effects of Background Coronal Conditions

AOGS (Asia Oceanic Geosciences Society) 12th Annual meeting, Singapore, 2-7 August 2015

170. West, M.; Zhukov, A.N.; Dolla, L.; Rodriguez, L.

Coronal Seismology Using EUV Waves: Estimation of the Coronal Magnetic Field Strength in the Quiet Sun

AOGS (Asia Oceanic Geosciences Society) 12th Annual meeting, Singapore, 2-7 August 2015

171. Yamauchi, M.; Dandouras, I.; Rathsmann, P. and the The NITRO Proposal Team

Nitrogen Ion TRacing Observatory (NITRO) ESA's M-class call

EGU General Assembly 2015, Vienna, Austria, 13-17 April 2015 (poster)

172. Yamauchi, M.; Dandouras, I.; Rathsmann, P.; De Keyser, J. and the NITRO proposal team

Nitrogen Ion TRacing Observatory (NITRO): A planetary mission to the Earth

European Planetary Science Congress 2015, La Cité des Congrès, Nantes, France, 27 September-02 October 2015

173. Yamauchi, M.; Dandouras, I.; Reme, H.; De Keyser, J. and the NITRO proposal team

Upgraded Nitrogen Ion TRacing Observatory (NITRO) for M5

25th Cluster Workshop (Cluster 15th and Double Star 10th anniversary workshop), Venice, Italy, 12-16 October 2015 (poster)

174. Zhukov, A.N.; Rodriguez, L.; Galano, D.; Mestreau-Garreau, A.; Zender, J.; Thizy, C.; Servaye, J.-S.

ASPIICS, a Giant Solar Coronagraph Onboard the PROBA-3 Mission

Measurement Techniques in Solar and Space Physics, NCAR, Boulder, Colorado, USA, 20-24 April 2015

Public Outreach: Talks and publications for the general public

1. Andries, J.
Space Weather Services @ Belgian Space Pole: Institutional and organisational context
NATO visit to ROB, Brussels, Belgium, 26 February 2015
2. Bergeot, N.
Ionospheric monitoring
NATO visit to ROB, Brussels, Belgium, 26 February 2015
3. Berghmans, D.
Observational infrastructure at Brussels Space Pole
NATO visit to ROB, Brussels, Belgium, 26 February 2015
4. Berghmans, D.
Operationele Directie Zonnewetenschap en Ruimtetuurgang
Presentation during visit of State Secretary Sleurs to ROB, 19 May 2015
5. Borremans, K.; Lemaire, J.; Pierrard, V.; Lopez Rosson, G.
The radiation belts of the Earth
KU Leuven seminar, Leuven, Belgium, 6 October 2015
6. Clette, F.
L'activité solaire: source et instabilités
Université de Mons (visiting students), ROB, Brussels, Belgium, 28 April 2015
7. Clette, F.
Redécouverte de 400 ans d'observations de l'activité solaire
Société Astronomique de Liège, Liège, Belgium, 23 November 2015
8. Clette, F.
Un nouveau regard sur 400 ans d'observation de l'activité solaire
Société Royale Belge d'Astronomie, ROB, Brussels, Belgium, 16 December 2015
9. Cuypers, J.; Katsiyannis, A.C.
Observatorio Real de Bélgica: ¿se puede estudiar el sol entre tanta nube?
Planeta Espuni Website, 20 November 2015
10. De Keyser, J.; Equeter, E.
De planeterella - emissie in TL-lampen, poollicht, en kometen
Demonstraties tijdens de ESERO Rosetta-event, BIRA-IASB, Brussels, Belgium, 7 May 2015
11. De Keyser, J.
Poollicht: een blik achter het optische verschijnsel
Poollichtdag, Volkssterrenwacht Urania, Hove, Belgium, 27 September 2015
12. De Keyser, J.
Planeterella demonstrations
Visit of students from German-speaking primary schools, BIRA-IASB, Brussels, Belgium, 13 November 2015
13. Devos, A.
SIDC: Operational Software & Products
NATO visit to ROB, Brussels, Belgium, 26 February 2015
14. Devos, A.
Today's SW forecast
Visit Met Office to ROB, Brussels, Belgium, 2 October 2015
15. D'Huys, E.
Ruimtetuurgang en PROBA2
Junior College sessions, KU Leuven Campus Heverlee, Belgium, 8 January 2015
16. D'Huys, E.; Janssens, J.; Vanlommel, P.
Solar eclipse of 20 March (support of public event)
Planetarium, Brussels, Belgium, 20 March 2015
17. Dierckxsens, M.; Crosby, N.
Solar Energetic Particle (SEP) events
NATO visit to ROB, Brussels, Belgium, 26 February 2015
18. Dolla, L.; Mestdag, P.
Expérience de classe avec Spirulina - les résultats
SCK-CEN, Mol, Belgium, 23 April 2015
19. Janssens, J.; Vanlommel, P.; Verbeeck, C.; Berghmans, D.
Onderzoek naar de zonnecorona
Zenit, pp. 30-31, March 2015
20. Janssens, J.
Het voorspellen van zonnevlammen
PROBA2@school sessions for high school students, Klein Seminarie, Hoogstraten, Belgium, 31 March 2015
21. Janssens, J.
De kunst van het zonnewaarnemen
MIRA Public Observatory, Grimbergen, Belgium, 15 April 2015
22. Janssens, J.
Zon en Ruimtetuurgang
Zonnekijkdag 2015, Planetarium, Brussels, Belgium, 5 July 2015
23. Janssens, J.; Rodriguez, L.; the SIDC forecasters team

- Forecasting of geomagnetic storms*
Visit Met Office to ROB, Brussels, Belgium, 2 October 2015
24. Janssens, J.
De nieuwe kleren van het zonnevlekkengetal
Bijeenkomst Nederlandse Werkgroep Zon, Utrecht, The Netherlands, 3 October 2015
25. Janssens, J.
Het SIDC: de voorspelling van het ruimteweer
Symposium NVBM, Wageningen, The Netherlands, 20 November 2015
26. Janssens, J.
Space weather predictions for space missions
ESWW12 (Tutorial), Oostende, Belgium, 23-27 November 2015
27. Kraaikamp, E.
Solar Demon - detecting flares, dimmings and EUV waves (in near real-time on SDO/AIA images)
Visit Met Office to ROB, Brussels, Belgium, 2 October 2015
28. Malisse, V.
Staff (Demo)
Visit Met Office to ROB, Brussels, Belgium, 2 October 2015
29. Magdalenic, J.
Type II radio bursts and their association with CME/flare events
Visit Met Office to ROB, Brussels, Belgium, 2 October 2015
30. Magdalenic, J.
Mapping the 3D position of solar coronal shock wave on 05 March 2012 using radio triangulation
Visit Met Office to ROB, Brussels, Belgium, 2 October 2015
31. Martinez Picar, A.
5 historias por las que 2015 fue un año extraordinario en exploración espacial
BBC Mundo Website, 30 December 2015
32. Rodriguez, L.
Forecasting of geomagnetic storms
NATO visit to ROB, Brussels, Belgium, 26 February 2015
33. Stegen, K.
PROBA2: Ontwikkeling, lancering en exploitatie
PROBA2@school sessions for high school students, Klein Seminarie, Hoogstraten, Belgium, 31 March 2015
34. Vanlommel, P.
Space Weather and its Impact
NATO visit to ROB, Brussels, Belgium, 26 February 2015
35. Vanlommel, P.
Wanneer de zon zich opwindt
Elcker-ik, Antwerpen, Belgium, 3 March 2015
36. Vanlommel, P.
Zonsverduistering 20 maart 2015
Service-flats Molenhof, Leuven, Belgium, 24 March 2015
37. Vanlommel, P.
Wat is Ruimteweer?
PROBA2@school sessions for high school students, Klein Seminarie, Hoogstraten, Belgium, 31 March 2015
38. Vanlommel, P.
De snelheid van een plasma wolk berekenen
PROBA2@school sessions for high school students, Klein Seminarie, Hoogstraten, Belgium, 31 March 2015
39. Vanlommel, P.
Grillen van de Zon & PROBA2
Vereniging voor Natuurkunde, Gent, Belgium, 2 April 2015
40. Vanlommel, P.
Zonnedata
Art-science dialog at MHKA, Antwerpen, Belgium, 20 June 2015
41. Vanlommel, P.
Ruimteweer en waarnemen met PROBA2 en PROBA3
VVS Zomerschool in Groep T, Leuven, Belgium, 24 August 2015
42. Verbeeck, C.; Gissot, S.; Berghmans, D.; Stegen, K.; Kraaikamp, E.; Giordanengo, B.; BenMoussa, A.
Au plus près du Soleil. Solar Orbiter, première mission vers le Soleil
Science Connection, 49, pp. 40-44, December 2015
43. Verbeeck, C.; Gissot, S.; Berghmans, D.; Stegen, K.; Kraaikamp, E.; Giordanengo, B.; BenMoussa, A.
De Zon - Van dichterbij dan ooit. Solar Orbiter, eerste missie naar de Zon
Science Connection, 49, pp. 40-44, December 2015

List of abbreviations

3D	Three dimensional	C-class flare	Common x-ray flare
AAS	American Astronomical Society	CACTus	Computer Aided CME Tracking software
ABOVE	Array for Broadband Observations of VLF/ELF Emissions	CALLISTO	Compound Astronomical Low frequency Low cost Instrument for Spectroscopy and Transportable Observatory
ACE	Advanced Composition Explorer	CCD	Charge-Coupled Device
ADU	Analog to Digital Units	CMMC	Community Coordinated Modeling Center
AFFECTS	Advanced Forecast For Ensuring Communications Through Space	CEN	Centre d'étude de l'énergie nucléaire
AGU	American Geophysical Union	CESRA	Community of European Solar Radio Astronomers
AIA	Atmospheric Imaging Assembly (SDO)	CGU	Canadian Geophysical Union
AIAA	American Institute of Aeronautics and Astronautics	CH	Coronal Hole
ALC	Automatic LIDAR Ceilometer	CHARM	Contemporary physical challenges in Heliospheric and AstRophysical Models
AOGS	Asia Oceania Geosciences Society	CIOMP	Changchun Institute of Optics, fine Mechanics and Physics (China)
APWC	Antennas and Propagation in Wireless communications	Cluster	ESA/NASA mission to study the Earth's magnetosphere (no acronym)
AR	Active Region	CMA	China Meteorological Administration
ASGARD	An educational space program for schools (no acronym)	CME	Coronal Mass Ejection
ASPIICS	Association of Spacecraft for Polarimetric and Imaging Investigation of the Corona of the Sun (PROBA-3)	CMOS	Complementary Metal Oxide Semiconductor
AT-RASC	Atlantic Radio Science Conference	COMESSEP	COronal Mass Ejections and Solar Energetic Particles
ATM	Air Traffic Management	COPUOS	COmmittee on the Peaceful Uses of Outer Space (UN)
AU	Astronomical Unit; about 150 million km	COR (1/2)	Coronagraph (Inner/Outer) onboard STEREO
BBC	British Broadcasting Corporation	CORDEX	Coordinated Regional climate Downscaling Experiment
BBC-SWS	Balkan, Black Sea, and Caspian Sea Regional Network on Space Weather Studies	COSPAR	COmmittee on SPACe Research
BELSPO	Belgian Science Policy Office	COST	(European) COoperation in Science & Technology
BIRA	Belgisch Instituut voor Ruimte-Aëronomie	CSL	Centre Spatial de Liège
BISA	Belgian Institute for Space Aeronomy	CSPM	Coimbra Solar Physics Meeting
BRAMS	Belgian RAdio Meteor Stations	CubeSat	A small satellite measuring 10cm x 10cm x 10cm
B.USOC	Belgian User Support and Operation Center	D2D	Digisonde-to-Digisonde
Bz	Component of the IMF perpendicular to the ecliptic ("north-south" component)		

DIARAD	Differential Absolute RADiometer	EUI	Extreme-Ultraviolet Imagers (Solar Orbiter)
DN	Digital Number (pixel values not calibrated into physically meaningful units)	EUMETNET	European Meteorological services Network
DOI	Digital Object Identifier	EUMETSAT	European Organization for the Exploitation of Meteorological Satellites
DPM	Data Processing Model		
DPS	Digital Portable Sounder	EUREF	EUropean Reference Frame
DSCOVER	Deep Space Climate Observatory	EUV	Extreme Ultraviolet
DSLPL	Dual Segmented Langmuir Probe (PROBA2)	EUVI	Extreme Ultraviolet Imager (STEREO/SECCHI)
Dst	Disturbance Storm Time index	EVE	Extreme ultraviolet Variability Experiment (SDO)
E-GVAP	EUMETNET EIG GNSS water VApour Program	F _{10.7 cm}	Solar radio flux at 10.7 cm wavelength
ECA	European Cockpit Association	F ₂	Main ionospheric layer
ECMWF	European Centre for Medium- range Weather Forecasts	FAS	Frequency and Angular Sounding
Eds.	Editors	FLIP	FLuid Implicit Particle
EGU	European Geosciences Union	foF2	Critical frequency F2-layer
EISCAT	European Incoherent SCATter scientific association	FOV	Field-Of-View
EIT	Extreme ultraviolet Imaging Telescope (SOHO)	FP7	Framework Program 7 (EU)
ELF	Extremely Low Frequency	FSL	Fluid Science Laboratory
ENEON	European Network of Earth Observation Networks (H2020)	FST	Facility Science Team (ISS- SOLAR)
EPN	EUREF Permanent Network	GCOS	Global Climate Observing System
EPT	Energetic Particle Telescope (PROBA-V)	GeV	Giga electronvolt ($10^9 \cdot 1.6 \cdot 10^{-19}$ Joule)
ERA	ECMWF re-analysis	GHz	Gigahertz (10^9 Hz)
ERB	Earth Radiation Budget	GNSS	Global Navigation Satellite System
ES	Earth System (Science and Environmental Management (COST)	GNSS4SWEC	Advanced GNSS tropospheric products for the monitoring of Severe Weather Events and Climate
ESA	European Space Agency	GOES	Geostationary Operational Environmental Satellite
ESAC	European Space Astronomy Centre	GOME	Global Ozone Monitoring experiment (SCIAMACHY)
ESERO	European Space Education Resource Office	GOMESCIA	GOME/SCIAMACHY/GOME-2
ESOC	European Space Operations Centre	GPS	Global Positioning System (USA)
ESTEC	European Space Research and Technology Centre	GRAPE	GNSS Research and Application for Polar Environment
ESWP	European Space Weather Portal	GRUAN	GCOS Reference Upper-Air Network
ESWW	European Space Weather Week	H	Hydrogen
EU	European Union	H-alpha (H α)	A red visible spectral line created by Hydrogen
Euhforia	European Heliospheric Forecasting Information Asset		

HEK	Heliophysics Events Knowledgebase	IRIS	Interface Region Imaging Spectrograph
HELCATS	HELiospheric Cataloguing, Analysis and Techniques Service	ISBN	International Standard Book Number
HF	High Frequency	ISS	International Space Station
HI	Heliospheric Imager (STEREO)	ISSI	International Space Science Institute
$h_m F_2$	peak density height of F ₂ -layer	IT	Information Technology
HMI	Heliospheric and Magnetic Imager (SDO)	IUGG	International Union of Geodesy and Geophysics
HSRS	Humain Solar Radio Spectrograph	IWV	Integrated Water Vapour
HuRAS	Humain Radio Astronomy Station	jHV	jHelioViewer
Hz	Hertz (per second)	JSWSC	Journal of Space Weather and Space Climate
IAIN	International Association of Institutes of Navigation	KAW	Kinetic Alfvén Waves
IAS(B)	Institut d'Aéronomie Spatiale de Belgique	K _p	A geomagnetic index, ranging from 0 (quiet) to 9 (extremely severe storm)
IAU	International Astronomical Union	KSB	Koninklijke Sterrenwacht van België
ICEAA	International Conference on Electromagnetics in Advanced Applications	KSP	Key Science Project
ICME	Interplanetary CME	KUL	Katholieke Universiteit Leuven
ICRC	International Cosmic Ray Conference	kV	kiloVolt (10 ³ Volt)
ICT	Information and Communication Technologies	λ	wavelength
IEEE	Institute of Electrical and Electronics Engineers	L	Letter
IES	Ionospheric Effects Symposium	L1	First Lagrangian point
IGS	International GNSS Service	LASCO	Large Angle Spectrometric Coronagraph (SOHO); small (C2) and wide (C3) field of view
IMC	International Meteor Conference	LDE	Long Duration Event
IMC	Inner Magnetosphere Coupling	LEO	Low Earth Orbit
IMO	International Meteor Organization	LIDAR	LIght Detection And Radar
IMF	Interplanetary Magnetic Field	LMSAL	Lockheed Martin Solar and Astrophysics Laboratory
ION	Institute Of Navigation	LOC	Local Organizing Committee
IPC	International Pyrheliometric Comparison	LOFAR	Low-Frequency Array
IPE	Ionosphere-Plasmasphere Electrodynamics	LOUI-Base	Lowell ObliqUe Incidence database
IPELS	Interrelationship between Plasma Experiments in the Laboratory and in Space	LT	Local Time
IPSL	Institut Pierre-Simon Laplace	LYRA	Lyman Alpha Radiometer (PROBA2)
IR	Infrared	LWS	Living With a Star
		μm	micrometer (10 ⁻⁶ meter)
		M-class	Medium class satellite
		M-class flare	Medium x-ray flare
		MADAWG	Modelling and Data Analysis Working Group (SoIo)
		MB	Megabyte
		MC	Management Committee

MeV	Mega electronvolt ($10^6 \cdot 1.6 \cdot 10^{-19}$ Joule)	PICASSO	Pico-satellite for Atmospheric and Space Science Observations
MHD	Magnetohydrodynamics		
MHKA	Museum van Hedendaagse Kunst Antwerpen	PMOD	Physikalisch-Meteorologisches Observatorium Davos
MHz	Megahertz ($10^6/s$)		
MSSL	Mullard Space Science Laboratory	PPP	Precise Point Positioning
NASA	National Aeronautics and Space Administration	PROBA	PRoject for OnBoard Autonomy
NATO	North-Atlantic Treaty Organization	PRODEX	PRogram for the Development of scientific Experiments
NCAR	National Center for Atmospheric Research	PTB	Physikalisch-technische Bundesanstalt
Ne	Neon	Q&A	Questions and Answers
Net-TIDE	Pilot Network for Identification of Travelling Ionospheric Disturbances in Europe	R&D	Research and Development
		RHESSI	Reuven Ramaty High Energy Solar Spectroscopic Imager
NIR	Near IR	RMI(B)	Royal Meteorological Institute (of Belgium)
NITRO	Nitrogen Ion TRacing Observatory (ESA)	ROB	Royal Observatory of Belgium
NM	Neutron Monitor	ROMA	Rank-Ordered Multifractal Analysis
nm	nanometer (10^{-9} meter)	RWC	Regional Warning Center
$N_m F_2$	peak density of F_2 -layer	S-band	Radio waves with frequencies ranging from 2 to 4 GHz (IEEE)
NOAA	National Oceanic and Atmospheric Administration (numbering of sunspots)	SACS	Support to Aviation Control Service
NOMAD	Nadir and Occultation for MArS Discovery (Exomars/TGO)	SC24	Solar Cycle 24
nT	nano-Tesla (10^{-9} Tesla)	SCAR	Scientific Committee on Antarctic Research
NVBM	Nederlandse Vereniging ter Bevordering van de Meteorologie	SCK	StudieCentrum voor Kernenergie
NWP	Numerical Weather Prediction	SCIAMACHY	SCanning Imaging Absorption spectroMeter for Atmospheric CHartography (ENVISAT)
O	Oxygen	SDO	Solar Dynamics Observatory
OI	Oblique Incidence	SECCHI	Sun Earth Connection Coronal and Heliospheric Investigation (STEREO)
ORB	Observatoire Royal de Belgique	SEP	Solar Energetic Particle
OSCAR	Observatories of the Solar Corona and Active Regions	SESAR	Single European Sky ATM Research
P2SC	PROBA2 Science Center	SFU, sfu	Solar Flux Unit ($10^{-22} W m^{-2} Hz^{-1}$)
PARAFOG	Predictive Alert of RAdiation FOG	SHINE	Solar Heliospheric
PFSS	Potential Field Source Surface		INterplanetary Environment
pfu	particle (proton) flux unit: the number of particles registered per second, per square cm, and per steradian	SHOCK	Solar and Heliospheric Collisionless Kinetics
PhD	Doctor of Philosophy	SIDC	Solar Influences Data analysis Center
PI	Principal Investigator		

SILSO	Sunspot Index and Long-term Solar Observations	STCE	Solar-Terrestrial Centre of Excellence
SIRTA	Site Instrumental de Recherche par Télédétection Atmosphérique (IPSL)	STEREO	Solar-TERrestrial RELations Observatory
SLP	Sweeping / Segmented / Single / Split / Spherical Langmuir Probe	STORM	Solar system plasma Turbulence: Observations, intermittency and Multifractals
SN	Sunspot Number	SWAP	Sun Watcher using APS detector and image Processing (PROBA2)
SN	Space weather and Near-earth objects	SWAVES	STEREO WAVES
SOC	Science Operations Centre	SWE	Space WEather
SOHO	SOLar & Heliospheric Observatory	SWSC	Space Weather and Space Climate journal
SOL-ACES	SOLar Auto-Calibrating Extreme ultraviolet and ultraviolet Spectrometers (ISS-SOLAR)	SWT	Science Working Team
SOLAR	ESA project onboard ISS (Columbus Laboratory), controlled by B.USOC, and having 3 main instruments: SOVIM, SOLSPEC and SOL-ACES	SWx	Space weather
		TEC	Total Electron Content
		TESS	Triennial Earth-Sun Summit
		TGO	Trace Gas Orbiter (Exomars)
		THESOW	Turbulence and Heating in the Solar Wind
		TID	Travelling Ionospheric Disturbance
SOLID	SOLar Irradiance Data exploitation (FP7)	TIM	Total Irradiance Monitor
Solo	Solar Orbiter	TL	Tube Luminescent
SOLSPEC	SOLar SPECTral irradiance measurements (ISS-SOLAR)	TOPROF	Towards Operational ground based PROFiling with ceilometers, doppler lidars and microwave radiometers for improving weather forecasts
SOLVAM	SOLar VARIability Monitor		
SORCE	Solar Radiation and Climate Experiment	TOR	Transmitters-of-Opportunity Reception
SOVIM	Solar Variations and Irradiance Monitor (ISS-SOLAR)	TSI	Total Solar Irradiance
SOWG	Science Operations Working Group	UHF	Ultra High Frequency
SP	Signal Processing	UK	United Kingdom
SPENVIS (-NG)	Space Environment Information System (- Next Generation)	UKUS	UK-Ukrain-Spain
sr	steradian	UNCOPUOS	United Nations Committee on the Peaceful Use of Outer Space
SREM	Standard Radiation Environment Monitor (Integral, Rosetta)	URSI	International Union of Radio Science – Union Radio-Scientifique Internationale
SSA	Space Situational Awareness	US(A)	United States (of America)
SSCC	SSA Space Weather Coordination Centre	USET	Uccle Solar Equatorial Table
SSN	SunSpot Number	USU	Utah State University
STAFF	Solar Timelines viewer for AFFECTS	UT(C)	(Coordinated) Universal Time
		UV	Ultraviolet
		UVIS	Ultraviolet and Visible
		V	Volt
		VHF	Very High Frequency

VI	Vertical Incidence	W/m ²	Watt per square meter
VIRGO	Variability of solar IRradiance and Gravity Oscillations	WAVES	Radio and plasma wave investigation (WIND, STEREO)
VISION	Visible Spectral Imager for Occultation and Nightglow	WDC	World Data Center
VKI	Von Karman Institute	WG	Working Group
VLF	Very Low Frequency	WP	Work Package
VSWMC	Virtual Space Weather Modelling Centre	WRC	World Radiation Center
VUB	Vrije Universiteit Brussel	WS	Workshop
VUV	Vacuum ultraviolet	X-class flare	Extreme x-ray flare
VVS	Vereniging Voor Sterrenkunde	ZTD	Zenith tropospheric Total Delays
W	Watt		